6192 *Inorg. Chem.* **2009**, *48*, 6192–6204
DOI: 10.1021/ic900522u

Inorganic Chemistry
Article

Tri-, Tetra-, and Hexanuclear Copper(II) Phosphonates Containing *N*-Donor Chelating Ligands: Synthesis, Structure, Magnetic Properties, and Nuclease Activity

Vadapalli Chandrasekhar,*,† Tapas Senapati,† E. Carolina Sañudo,‡ and R. Clérac§,||

†*Department of Chemistry, Indian Institute of Technology Kanpur, Kanpur-208016, India,* ‡*Departament de Química Inorgànica i, Institut de Nanociència i Nanotecnologia, Universitat de Barcelona, Diagonal 647, 08028 Barcelona, Spain,* §*CNRS, UPR 8641, Centre de Recherche Paul Pascal (CRPP), Equipe "Matériaux Moléculaires Magnétiques", 115 avenue du Dr. Albert Schweitzer, Pessac, F-33600, France, and* ||*Université de Bordeaux, UPR 8641, Pessac, F-33600, France*

Received March 17, 2009

Reaction of $Cu(ClO_4)_2 \cdot 6H_2O$ with cyclopentyl phosphonic acid and 2,2′-bipyridine (bpy) in presence of triethylamine afforded a trinuclear compound $[Cu_3(C_5H_9PO_3)_2(bpy)_3(MeOH)(H_2O)](ClO_4)_2$ (**2**). The latter dimerizes to a hexanuclear derivative $[Cu_6(C_5H_9PO_3)_4(bpy)_6(MeOH)_4](ClO_4)_4$ (**1**) under prolonged reaction conditions. Reaction of $CuCl_2$ with cyclopentyl phosphonic acid and 2,2′-bipyridylamine (bpya) affords a tetranuclear derivative $[Cu_4(C_5H_9PO_3)_2(\mu\text{-}Cl)_2(bpya)_4](Cl)_2, (MeOH)_2$ (**3**). Reaction of the latter with $NaClO_4$ also affords a trinuclear compound $[Cu_3(C_5H_9PO_3)_2(\mu\text{-}Cl)(bpya)_3(H_2O)](ClO_4)$ (**4**). Double and single-bridged hexanuclear species, $[\{Cu_3(C_5H_9PO_3)_2(bpy)_3(bpp)\}(MeOH)_2(H_2O)(CH_2Cl_2)(ClO_4)_2]_2$ (**5**), $[\{Cu_3(i\text{-}PrPO_3)_2(bpy)_3(4.4'\text{-}bpy)(H_2O)\}(H_2O)_2(ClO_4)_2]_2$ (**6**), $[\{Cu_3(C_5H_9PO_3)_2(bpya)_3(4.4'\text{-}bpy)(H_2O)\}(MeOH)(H_2O)(ClO_4)_2]_2$ (**7**), and $[Cu_6(t\text{-}BuPO_3)_4(phen)_6(4,4'\text{-}bpy)(MeOH)_4](CH_2Cl_2)(H_2O)(ClO_4)_4$ (**8**) (phen = 1,10-phenanthroline) were obtained by the reaction of an in situ generated trinuclear complex with appropriate bridging ligands 4,4′-bipyridine (4,4′-bpy) or 1,3-bis(4-pyridyl)propane (bpp). ESI-MS studies of these complexes reveal that **2**−**4** retain their structures in solution. Molecular structures of **2**−**8** were determined by X-ray crystallography. All the compounds reveal a capping coordination mode by tridentate phosphonate $[RPO_3]^{2-}$ ligands. Detailed magnetic studies on **2** and **4**−**8** reveal intramolecular antiferromagnetic interactions between Cu(II) $S = 1/2$ spins. **2** and **4** are excellent artificial nucleases and can convert supercoiled plasmid DNA (pBR322) into its nicked form without the aid of an external oxidant.

Introduction

Transition metal-phosphonate materials possessing extended structures[1] have been studied quite well in view of their interesting structures as well as their applications in diverse areas such as catalysis,[2] sorption,[3] cation-exchange,[4] sensors,[5] and non-linear optical properties.[6] More recently the field of molecular metal-phosphonate systems[7] has also been attracting interest. For a long time the preparation of

*To whom correspondence should be addressed. E-mail: vc@iitk.ac.in.

(1) (a) Clearfield, A. *Prog. Inorg. Chem.* **1998**, *47*, 371. (b) Inoue, A.; Shinokubo, H.; Oshima, K. *J. Am. Chem. Soc.* **2003**, *125*, 1484. (c) Thompson, M. E. *Chem. Mater.* **1994**, *6*, 1168. (d) Burkholder, E.; Golub, V.; O'Connor, C. J.; Zubieta, J. *Inorg. Chem.* **2004**, *43*, 7014. (e) Yang, B.-P.; Mao, J.-G. *Inorg. Chem.* **2005**, *44*, 566. (f) Amicangelo, J. C.; Leenstra, W. R. *Inorg. Chem.* **2005**, *44*, 2067. (g) Du, Z.-Y.; Xu, H.-B.; Mao, J.-G. *Inorg. Chem.* **2006**, *45*, 9780. (h) Taylor, J. M.; Mahmoudkhani, A. H.; Shimizu, G. K. H. *Angew.Chem., Int. Ed.* **2007**, *46*, 795. (i) Ouelette, W.; Koo, B. K.; Burkholder, E.; Golub, V.; Connor, C. J. O.; Zubieta, J. *Dalton Trans.* **2004**, 1527. (j) Khan, I.; Zubieta, J. *Prog. Inorg. Chem.* **1995**, *43*, 1. (k) Finn, R. C.; Zubieta, J. *Chem. Commun.* **2000**, 1321. (l) Cao, G.; Hong, H.-G.; Mallouk, T. E. *Acc. Chem. Res.* **1992**, *25*, 420.

(2) (a) Lassahn, P.-G.; Lozan, V.; Timco, G. A.; Christian, P.; Janiak, C.; Winpenny, R. E. P. *J. Catal.* **2004**, *222*, 260. (b) Fiedler, D.; Leung, D. H.; Bergman, R. G.; Raymond, K. N. *Acc. Chem. Res.* **2005**, *38*, 351. (c) Hu, A.; Yee, G. T.; Lin, W. *J. Am. Chem. Soc.* **2005**, *127*, 12486. (d) Nonglaton, G.; Benitez, I. O.; Guisle, I.; Pipeler, M.; Leger, J.; Dubreuil, D.; Tellier, C.; Talham, D. R.; Bujoli, B. *J. Am. Chem. Soc.* **2004**, *126*, 1497.

(3) (a) Gallagher, L. A.; Serron, S. A.; Wen, X.; Hornstein, B. J.; Dattelbaum, D. M.; Schoonover, J. R.; Meyer, T. J. *Inorg. Chem.* **2005**, *44*, 2089. (b) Maeda, K. *Microporous Mesoporous Mater.* **2004**, *73*, 47. (c) Fredoueil, F.; Massiot, D.; Janvier, P.; Gingl, F.; Bujoli-Doeuff, M.; Evian, M.; Clearfield, A.; Bujoli, B. *Inorg. Chem.* **1999**, *38*, 1831. (d) Maeda, K.; Kiyozumi, Y.; Mizukami, F. *J. Phys. Chem. B* **1997**, *101*, 4402. (e) Yue, Q.; Yang, J.; Li, G.-H.; Li, G.-D.; Chen, J.-S. *Inorg. Chem.* **2006**, *45*, 4431.

(4) (a) Alberti, G. *Acc. Chem. Res.* **1978**, *11*, 163. (b) Wang, J. D.; Clearfield, A.; Peng, G.-Z. *Mater. Chem. Phys.* **1993**, *35*, 208. (c) Zang, B.; Clearfield, A. *J. Am. Chem. Soc.* **1997**, *119*, 2751. (d) Clearfield, A. *Inorganic Ion Exchange Materials*; CRC Press: Boca Raton, FL, 1982. (e) Alberti, G. In *Comprehensive Supramolecular Chemistry*; Alberti, G., Bein, T., Eds.; Pergamon: New York, 1996; Vol. *7*, pp 151.

(5) (a) Du, Z.-Y.; Xu, H.-B.; Mao, J.-G. *Inorg. Chem.* **2006**, *45*, 6424. (b) Ungashe, S. B.; Wilson, W. L.; Katz, H. E.; Scheller, G. R.; Putvinski, T. M. *J. Am. Chem. Soc.* **1992**, *114*, 8717. (c) Sanchez- Moreno, M. J.; Fernandez-Botello, A.; Gomez-Coca, R. B.; Griesser, R.; Ochocki, J.; Kotynski, A.; Niclos-Gutierrez, J.; Moreno, V.; Sigel, H. *Inorg. Chem.* **2004**, *43*, 1311.

(6) (a) Ungashe, S. B.; Wilson, W. L.; Katz, H. E.; Scheller, G. R.; Putvinski, T. M. *J. Am. Chem. Soc.* **1992**, *114*, 8717. (b) Cabeza, A.; Aranda, M. A. G.; Bruque, S.; Poojary, D. M; Clearfield, A.; Sanz, J. *Inorg. Chem.* **1998**, *37*, 4168. (c) Zhang, B.; Poojary, D. M.; Clearfield, A. *Inorg. Chem.* **1998**, *37*, 249. (d) Ayyappan, P.; Evans, O. R.; Cui, Y.; Wheeler, K. A.; Lin, W. *Inorg. Chem.* **2002**, *41*, 4978.

(7) (a) Chandrasekhar, V.; Sasikumar, P.; Boomishankar, R.; Anantharaman, G. *Inorg. Chem.* **2006**, *45*, 3344. (b) Konar, S.; Bhuvanesh, N.; Clearfield, A. *J. Am. Chem. Soc.* **2006**, *128*, 9604. (c) Brechin, E. K.; Coxall, R. A.; Parkin, A.; Parsons, S.; Tasker, P. A.; Winpenny, R. E. P. *Angew. Chem., Int. Ed.* **2001**, *40*, 2700.

 Published on Web 06/05/2009

such compounds has remained a challenge in view of solubility problems. However, the use of ancillary ligands along with lipophilic phosphonic acids has allowed the isolation of a number of metal-phosphonate complexes.[8−14] Recently, we have found that the use of chelating nitrogen ligands such as 2,2′-bipyridine (bpy), 1,10-phenanthroline (phen), or 2,2′-bipyridylamine (bpya) allowed reasonable synthetic control, by blocking the coordination sites and thereby limiting reactive sites on the metal ion, to facilitate isolation of discrete molecular derivatives such as $[Cu_6(C_5H_9PO_3)_4(bpy)_6(MeOH)_4](ClO_4)_4]$ (**1**).[15] It may be noted that **1** consists of two trinuclear subunits that are joined by a Cu_2O_2 four-membered ring. Reducing the reaction time has now allowed us to isolate a trinuclear copper-phosphonate complex, $[Cu_3(C_5H_9PO_3)_2(bpy)_3(MeOH)(H_2O)](ClO_4)_2$ (**2**) possessing identical structure to that of the subunit in **1**. A structurally related trinuclear compound $[Cu_3(C_5H_9PO_3)_2(\mu\text{-}Cl)(bpya)_3(H_2O)](ClO_4)$ (**4**) could also be prepared by reaction of the tetranuclear derivative $[Cu_4(C_5H_9PO_3)_2(\mu\text{-}Cl)_2(bpya)_4](Cl)_2(CH_3OH)_2$ (**3**) with $NaClO_4$. Furthermore, by adopting a four-component reaction protocol involving a Cu(II) salt, alkylphosphonic acid, triethylamine, and 4,4′-bipyridine (4,4′-bpy) [or 1,3-bis(4-pyridyl)propane (bpp)], we have been able to isolate double and single-bridged hexanuclear complexes: $[\{Cu_3(C_5H_9PO_3)_2(bpy)_3(bpp)\}(MeOH)_2(H_2O)(CH_2Cl_2)(ClO_4)_2]_2$ (**5**), $[\{Cu_3(i\text{-}PrPO_3)_2(bpy)_3(4,4'\text{-}bpy)(H_2O)\}(H_2O)_2(ClO_4)_2]_2$ (**6**), $[\{Cu_3(C_5H_9PO_3)_2(bpya)_3(4,4'\text{-}bpy)(H_2O)\}(MeOH)(H_2O)(ClO_4)_2]_2$ (**7**), $[Cu_6(t\text{-}BuPO_3)_4(phen)_6(4,4'\text{-}bpy)(MeOH)_4](CH_2Cl_2)(H_2O)(ClO_4)_4$ (**8**). The magnetic behavior of **2**, **4**, **5**, **6**, **7**, **8**, and the nuclease activity of **2** and **4** are also reported herein. The nuclease activity of the hexanuclear compounds was not studied because they do not retain their integrity in solution (vide infra).

Experimental Section

Reagents and General Procedures. Solvents were purified by conventional methods.[16] The following chemicals and reagents were used as received: C_5H_9Cl (Aldrich, U.S.A), *i*-PrCl (s. d. Fine Chemicals, India), $Cu(ClO_4)_2\cdot 6H_2O$ (Fluka, Switzerland), 2,2′-bipyridine (bpy), 4,4′-bipyridine, 1,10-phenanthroline (phen), 1,3-bis(4-pyridyl)propane (bpp) (Aldrich, U.S.A), $AlCl_3$ (s. d. Fine Chemicals, India), PCl_3 (s. d. Fine Chemicals, India), supercoiled plasmid DNA (pBR322) (Bangalore Genei, India), ethidium bromide (LOBA Chemie Pvt. Ltd. Mumbai, India), sodium cacodylate buffer (SRL, Mumbai, India), ethylenediaminetetraacetic acid (EDTA), DMSO, *t*-butanol, and D-mannitol (s. d. Fine Chemicals, Mumbai, India). All buffer solutions were prepared using Millipore water. The phosphonic acids $C_5H_9P(O)(OH)_2$, *i*-PrP(O)$(OH)_2$, and *t*-Bu(O)$(OH)_2$ were prepared by known literature procedures.[17]

Instrumentation. Melting points were measured using a JSGW melting point apparatus and are uncorrected. Electronic spectra were recorded on a Perkin-Elmer-Lambda 20 UV−vis spectrometer and on a Shimadzu UV-160 spectrometer using methanol as the solvent. IR spectra were recorded as nujol mulls on a Bruker Vector 22 FT IR spectrophotometer operating from 400 to 4000 cm^{-1}. ESI-MS analyses were performed on a Waters Micromass Quattro Micro triple quadrupole mass spectrometer. Electrospray ionization mechanism was used in positive ion full scan mode employing methanol as the solvent and nitrogen gas for desolvation. Capillary voltage was maintained at 3 kV and cone voltage was kept at 30 V. The temperature maintained for ion source was 100 °C and for desolvation 250 °C. ^1H and $^{31}P\{^1H\}$ NMR spectra were recorded in $CDCl_3$ solutions on a JEOL JNM LAMBDA 400 model spectrometer operating at 400.0 and 161.7 MHz respectively. Chemical shifts are reported in ppm and are referenced with respect to internal tetramethylsilane (^1H) and external 85% H_3PO_4 (^{31}P). Elemental analyses were carried out using a Thermoquest CE instruments CHNS-O, EA/110 model elemental analyzer.

Magnetic Measurements. The magnetic susceptibility measurements for **2** and **4** were obtained on polycrystalline samples with the use of a Quantum Design SQUID magnetometer MPMS-XL housed at the Centre de Recherche Paul Pascal. This magnetometer works between 1.8 and 400 K for direct current (dc) applied fields ranging from −7 to 7 T. Magnetic data for **5**−**8** were collected at the Unitat de Mesures Magnètiques at the Universitat de Barcelona using crushed crystals of the samples on a Quantum Design MPMS-XL SQUID magnetometer equipped with a 5 T magnet. The data for all the compounds were corrected for TIP, and the diamagnetic corrections were calculated using Pascal's constants; an experimental correction for the sample holder was applied.

Synthesis. General Procedure for 2−3. A mixture of $CuX_2\cdot nH_2O$ (X=Cl^-, ClO_4^-), phosphonic acid, and triethylamine was stirred in methanol (30 mL) for 4 h. A green-colored turbid solution was formed. To this reaction mixture was added an ancillary ligand (bpy, bpya) in CH_2Cl_2, and the reaction mixture stirred for a further 3 h. A clear solution that resulted was concentrated to 15 mL, filtered, and left undisturbed to allow crystallization.

$[Cu_3(C_5H_9PO_3)_2(bpy)_3(MeOH)(H_2O)](ClO_4)_2$ (2). Quantities: $Cu(ClO_4)_2\cdot 6H_2O$ (0.200 g, 0.540 mmol), cyclopentylphosphonic

(8) (a) Chandrasekhar, V.; Kingsley, S. *Angew. Chem., Int. Ed.* **2000**, *39*, 2320. (b) Chandrasekhar, V.; Kingsley, S.; Vij, A.; Lam, K. C.; Rheingold, A. L. *Inorg. Chem.* **2000**, *39*, 3238. (c) Anantharaman, G.; Walawalkar, M. G.; Murugavel, R.; Gábor, B.; Regine, H.-I.; Baldus, M.; Angerstein, B.; Roesky, H. W. *Angew. Chem., Int. Ed.* **2003**, *42*, 4482. (d) Chakraborty, D.; Chandrasekhar, V.; Bhattacharjee, M.; Krätzner, R.; Roesky, H. W.; Noltemeyer, M.; Schmidt, H.-G. *Inorg. Chem.* **2000**, *39*, 23.

(9) (a) Langley, S.; Helliwell, M.; Raftery, J.; Tolis, E. I.; Winpenny, R. E. P. *Chem. Commun.* **2004**, 142. (b) Maheswaran, S.; Chastanet, G.; Teat, S. J.; Mallah, T.; Sessoli, R.; Wernsdorfer, W.; Winpenny, R. E. P. *Angew. Chem., Int. Ed.* **2005**, *44*, 5044. (c) Tolis, E. I.; Helliwell, M.; Langley, S.; Raftery, J.; Winpenny, R. E. P. *Angew. Chem., Int. Ed.* **2003**, *42*, 3804. (d) Langley, S. J.; Helliwell, M.; Sessoli, R.; Rosa, P.; Wernsdorfer, W.; Winpenny, R. E. P. *Chem. Commun.* **2005**, 5029.

(10) (a) Kontturi, M.; Laurilla, E.; Mattsson, R.; Peräniemi, S.; Vepsäläinen, J. J.; Ahlgr.en, M. *Inorg. Chem.* **2005**, *44*, 2400. (b) Mehring, M.; Guerrero, G.; Dahan, F.; Mutin, P. H.; Vioux, A. *Inorg. Chem.* **2000**, *39*, 3325. (c) Otieno, T.; Mokry, L. M.; Bond, M. R.; Carrano, C. J.; Dean, N. S. *Inorg. Chem.* **1996**, *35*, 850. (d) Clarke, R.; Latham, K.; Rix, C.; Hobday, M.; White, J. *CrystEngComm* **2004**, *6*, 42. (e) Clarke, R.; Latham, K.; Rix, C.; Hobday, M.; White, J. *CrystEngComm* **2005**, *7*, 28. (f) Yao, H.-C.; Li, Y.-Z.; Zheng, L.-M; Xin, X.-Q. *Inorg. Chim. Acta* **2005**, *358*, 2523. (g) Yao, H.-C.; Li, Y.-Z.; Gao, S.; Song, Y.; Zheng, L.-M.; Xin, X.-Q. *J. Solid State Chem.* **2004**, *177*, 4557. (h) Zhao, Q.-H.; Du, L.; Fang, R.-B. *Acta Crystallogr.* **2006**, *E62*, m219. (i) Plutner, J.; Rohovec, J.; Kotek, J.; Zak, Z.; Lukeś, I. *Inorg. Chim. Acta* **2002**, *335*, 27.

(11) (a) Chandrasekhar, V.; Kingsley, S.; Hatigan, B.; Lam, M. K.; Rheingold, A. L. *Inorg. Chem.* **2002**, *41*, 1030.

(12) (a) Chandrasekhar, V.; Nagarajan, L.; Gopal, K.; Baskar, V.; Kögerler, P. *Dalton Trans.* **2005**, 3143. (b) Chandrasekhar, V.; Nagarajan, L.; Clérac, R.; Ghosh, S.; Senapati, T.; Verma, S. *Inorg. Chem.* **2008**, *47*, 5347. (c) Chandrasekhar, V.; Nagarajan, L.; Clérac, R.; Ghosh, S.; Verma, S. *Inorg. Chem.* **2008**, *47*, 1067.

(13) Langley, S.; Helliwell, M.; Sessoli, R.; Teat, S. J.; Winpenny, R. E. P. *Inorg. Chem.* **2008**, *47*, 497.

(14) Baskar, V.; Shanmugam, M.; Sañudo, E. C.; Shanmugam, M.; Collison, D.; McInnes, E. J. L.; Wei, Q.; Winpenny, R. E. P. *Chem. Commun.* **2007**, 37.

(15) Chandrasekhar, V.; Senapati, T.; Sanudo, E. C. *Inorg. Chem.* **2008**, *47*, 9553.

(16) *Vogel's Textbook of Practical Organic Chemistry*, 5th ed.; Longman: London, 1989.

(17) (a) Crofts, P. C.; Kosolapoff, G. M. *J. Am. Chem. Soc.* **1953**, *75*, 3379. (b) Bengelsdorf, I. S.; Barron, L. B. *J. Am. Chem. Soc.* **1955**, *77*, 2869.

acid (0.054 g, 0.360 mmol), triethylamine (0.110 g, 1.070 mmol), and 2,2′-bipyridine (bpy) (0.107 g, 0.540 mmol) .

Yield: 0.178 g, 82.3% (based on metal). Mp: 290 °C (d). UV−vis (CH_3OH) λ_{max}/nm (ε/L mol^{-1} cm^{-1}): 664 (186). FT-IR ν/cm^{-1}: 3475 (b), 3111 (m), 2923 (s), 2853 (s), 1600 (s), 1462 (s), 1377 (s), 1311 (m), 1253 (w), 1089 (b), 772 (m), 729 (m), 660 (w), 616 (w), 556 (w), 459 (w). ESI-MS m/z, ion: 478.5 $[Cu_3(C_5H_9PO_3)_2(bpy)_3]^{2+}$, 735.06 $[Cu_2(bpy)_2(C_5H_9PO_3)_2+H]^+$, 368.03 $[Cu(C_5H_9PO_3H)(bpy)]^+$, 375.06 $[Cu(C_{10}H_8N_2)_2]^+$, 218.98 $[Cu(bpy)]^+$. Anal. Calcd for $C_{41}H_{48}C_{12}Cu_3N_6O_{16}P_2$: C, 40.9; H, 4.02; N, 6.98. Found: C, 41.1; H, 4.26; N, 6.38.

$[Cu_4(C_5H_9PO_3)_2(\mu\text{-}Cl)_2(bpya)_4](Cl)_2(CH_3OH)_2$ (3). Quantities: $CuCl_2$ (0.200 g, 1.490 mmol), cyclopentylphosphonic acid (0.150 g, 1.00 mmol), triethylamine (0.202 g, 2.00 mmol), and 2,2′-bipyridylamine (bpya) (0.233 g, 1.480 mmol).

Yield: 0.387 g, 72.6% (based on metal). Mp: 280 °C (d). UV−vis (CH_3OH) λ_{max}/nm (ε/L mol^{-1} cm^{-1}): 685 (186). FT-IR ν/cm^{-1}: 2924 (s), 2854 (s), 1653 (m), 1584 (m), 1534 (s), 1464 (s), 1377 (s), 1267 (w), 1239 (m), 1116(s), 1037 (s), 1010 (m), 771 (s), 648 (w), 563 (w), 534 (w), 463 (w), 428 (w). ESI-MS m/z, ion: 653.007 $[Cu_4(C_5H_9PO_3)_2(\mu\text{-}Cl)_2(bpya)_4]^{2+}$, 765.075 $[Cu_2(C_5H_9PO_3)_2(bpya)]^+$, 383.03 $[Cu(C_5H_9PO_3H)(bpya)]^+$, 235.016 $[Cu(bpya)]^+$. Anal. Calcd for $C_{52}H_{62}Cl_4Cu_4N_{12}O_8P_2$: C, 43.3; H, 4.34; N, 11.7. Found: C, 44.9; H, 5.56; N, 10.8.

$[Cu_3(C_5H_9PO_3)_2(\mu\text{-}Cl)(bpya)_3(H_2O)](ClO_4)$ (4). A mixture of anhydrous $CuCl_2$ (0.200 g, 1.490 mmol), cyclopentylphosphonic acid (0.150 g, 1.00 mmol), and triethylamine (0.202 g, 2.00 mmol) was stirred in methanol (30 mL) for 6 h resulting in a green-colored turbid solution. To this was added 2,2′-bipyridylamine (bpya) in CH_2Cl_2 (10 mL) (0.233 g, 1.480 mmol) and stirred for a further 12 h affording a clear blue-colored solution. To this was added $NaClO_4$ (0.183 g, 1.490 mmol) and stirred for another 4 h. The reaction mixture was concentrated to 15 mL, filtered, and left undisturbed to allow crystallization. After 3−4 days blue-colored crystalline blocks of **4** were obtained.

Yield: 0.358 g, 64.7% (based on metal). Mp: 275 °C (d). UV−vis (CH_3OH) λ_{max}/nm (ε/L mol^{-1} cm^{-1}): 679 (186). FT-IR ν/cm^{-1}: 3411 (b), 2923 (s), 2854 (s), 1642 (s), 1586 (m), 1532 (m), 1466 (s), 1376 (s), 1240 (m), 1160 (m), 1112 (s), 1019 (m), 985 (m), 770 (s), 648 (w), 623 (m), 595 (m), 535 (m), 468 (w), 432 (w). ESI-MS m/z, ion: 1054.0 $[Cu_3(C_5H_9PO_3)_2(\mu\text{-}Cl)(bpya)_3(H_2O)]^+$, 383.04 $[Cu(C_5H_9PO_3H)(bpya)]^+$, 405.08 $[Cu(bpya)_2]^+$, 234.01 $[Cu(bpya)]^+$. Anal. Calcd for $C_{40}H_{47}Cl_2Cu_3N_9O_{11}P_2$: C, 41.7; H, 4.11; N, 10.9. Found: C, 41.9; H, 4.56; N, 10.5.

General Procedure for 5−8. A mixture of $Cu(ClO_4)_2\cdot 6H_2O$, phosphonic acid, and triethylamine was stirred in methanol (30 mL) for 4 h. A green-colored turbid solution was formed. To this reaction mixture was added an ancillary ligand (bpy, bpya, phen) in CH_2Cl_2, and the reaction mixture stirred for a further 3 h. A clear solution obtained. At this stage, a linker (4,4′-bipyridine, bpp) was added, and the reaction mixture stirred for another 6 h. This was concentrated to 15 mL, filtered, and left undisturbed to allow crystallization.

$[\{Cu_3(C_5H_9PO_3)_2(bpy)_3(bpp)\}(MeOH)_2(H_2O)(CH_2Cl_2)(ClO_4)_2]_2$ (5). Quantities: $Cu(ClO_4)_2\cdot 6H_2O$ (0.200 g, 0.540 mmol), cyclopentylphosphonic acid (0.054 g, 0.360 mmol), triethylamine (0.110 g, 1.070 mmol), 2,2′-bipyridine (0.085 g, 0.540 mmol), and 1,3-bis-(4-pyridyl)propane (bpp) (0.107 g, 0.270 mmol).

Yield: 0.175 g, 68.0% (based on metal). Mp: 272 °C (d). UV−vis (CH_3OH) λ_{max}/nm (ε/L mol^{-1} cm^{-1}): 667 (186). FT-IR ν/cm^{-1}: 2924 (s), 2854 (s), 1598 (m), 1460 (s), 1377 (s), 1090 (m), 730 (m), 622 (m). ESI-MS m/z, ion: 477.52 $[Cu_3(C_5H_9PO_3)_2(bpy)_3]^{2+}$, 735.06 $[Cu_2(bpy)_2(C_5H_9PO_3)_2+H]^+$, 368.02 $[Cu(C_5H_9PO_3H)(bpy)]^+$, 218.98 $[Cu(bpy)]^+$. Anal. Calcd for $C_{106}H_{112}Cl_4Cu_6N_{16}O_{28}P_4$: C, 47.1; H, 4.17; N, 8.28. Found: C, 47.5; H, 4.46; N, 8.34.

$[\{Cu_3(i\text{-}PrPO_3)_2(bpy)_3(4.4'\text{-}bpy)(H_2O)\}(H_2O)_2(ClO_4)_2]_2$ (6). Quantities: $Cu(ClO_4)_2\cdot 6H_2O$ (0.20 g, 0.54 mmol), isopropylphosphonic acid (0.045 g, 0.360 mmol), triethylamine (0.110 g, 1.070 mmol), 2,2′-bipyridine (0.085 g, 0.540 mmol), and 4,4′-bipyridine, (0.043 g, 0.270 mmol).

Yield: 0.183 g, 77.5% (based on metal). Mp: 285 °C (d). UV−vis (CH_3OH) λ_{max}/nm (ε/L mol^{-1} cm^{-1}): 666 (186). FT-IR ν/cm^{-1}: 2924 (s), 2854 (s), 1598 (m), 1461 (s), 1377 (s), 1308 (w), 1107 (s), 812 (w), 768 (m), 731(m), 622 (m), 462 (w). ESI-MS m/z, ion: 451.49 $[Cu_3(C_3H_7PO_3)_2(bpy)_3]^{2+}$, 683.02 $[Cu_2(bpy)_2(C_3H_7PO_3)_2+H]^+$, 342.0 $Cu[(C_3H_7PO_3H)(C_{10}H_8N_2)]^+$, 375.06 $[Cu(bpy)_2]^+$, 218.98 $[Cu(bpy)]^+$. Anal. Calcd for $C_{92}H_{96}Cl_4Cu_6N_{16}O_{30}P_4$: C 43.3; H, 3.79; N, 8.78. Found: C, 43.5; H, 3.86; N, 8.63.

$[\{Cu_3(C_5H_9PO_3)_2(bpya)_3(4.4'\text{-}bpy)(H_2O)\}(MeOH)(H_2O)(ClO_4)_2]_2$ (7). Quantities: $Cu(ClO_4)_2\cdot 6H_2O$ (0.200 g, 0.540 mmol), cyclopentylphosphonic acid (0.054 g, 0.360 mmol), triethylamine (0.110 g, 1.070 mmol), 2,2′-bipyridylamine (0.093 g, 0.540 mmol), 4,4′-bipyridine, (0.043 g, 0.270 mmol).

Yield: 0.167 g, 65.3% (based on metal). Mp: 285 °C (d). UV−vis (CH_3OH) λ_{max}/nm (ε/L mol^{-1} cm^{-1}): 670 (186). FT-IR ν/cm^{-1}: 3179 (b), 2924 (s), 2854 (s), 1674 (w), 1584 (m), 1539 (w), 1461 (s), 1377 (s), 1240 (w), 1157 (w), 1107 (s), 1055 (m), 1012 (m), 965 (m), 829 (w), 763 (m), 654 (w), 520 (w), 498 (w), 422 (w). ESI-MS m/z, ion: 501.24 $[Cu_3(C_5H_9PO_3)_2(bpya)_3]^{2+}$, 765.07 $[Cu_2(bpya)_2(C_5H_9PO_3)_2+H]^+$, 383.02 $[Cu(C_5H_9PO_3H)(C_{10}H_9N_3)]^+$, 405.08 $[Cu(bpya)_2]^+$, 233.99 $[Cu(bpya)]^+$. Anal. Calcd for $C_{100}H_{110}Cl_4Cu_6N_{22}O_{30}P_4$: C, 43.7; H, 4.04; N, 11.2. Found: C, 43. 8; H, 4.16; N, 11.0.

$[Cu_6(t\text{-}BuPO_3)_4(phen)_6(4,4'\text{-}bpy)(MeOH)_4](CH_2Cl_2)(H_2O)(ClO_4)_4$ (8). Quantities: $Cu(ClO_4)_2\cdot 6H_2O$ (0.200 g, 0.540 mmol), *tert*-butylphosphonic acid (0.075 g, 0.360 mmol), triethylamine (0.110 g, 1.070 mmol), 1,10-phenanthroline (0.107 g, 0.540 mmol), and 4,4′-bipyridine, (0.043 g, 0.270 mmol).

Yield: 0.168 g, 67.2% (based on metal). Mp: 292 °C (d). UV−vis (CH_3OH) λ_{max}/nm (ε/L mol^{-1} cm^{-1}): 674 (186). FT-IR ν/cm^{-1}: 3378 (b), 2924 (s), 2854 (s), 1595 (m), 1460 (s), 1377 (s), 1265 (w), 1221 (w), 1089 (s), 989 (m), 871 (w), 852 (m), 723 (s), 645 (w), 621 (m), 506 (w), 428 (w). ESI-MS m/z, ion: 501.5 $[Cu_3(phen_2)_3(C_4H_9PO_3)_2]^{2+}$, 759.04 $[Cu_2(phen_2)_2(C_4H_9PO_3)_2+H]^+$, 380.02 $[Cu(C_4H_9PO_3H)(phen)]^+$, 423.05 $[Cu(phen)_2]^+$, 242.98 $[Cu(phen)]^+$. Anal. Calcd for $C_{102}H_{108}Cl_4Cu_6N_{14}O_{32}P_4$: C, 45.6; H, 4.05; N, 7.29. Found: C, 45.7; H, 4.06; N, 7.35.

X-ray Crystallography. The crystal data and the cell parameters for compounds **2**−**8** are given in Tables 1 and 2. Single crystals suitable for X-ray crystallographic analyses were obtained by slow evaporation of methanol/dichloromethane mixture (**2**−**8**). The crystal data for compounds **2**−**8** have been collected on a Bruker SMART CCD diffractometer using a Mo Kα sealed tube. The program SMART[18a] was used for collecting frames of data, indexing reflections, and determining lattice parameters, SAINT[18a] for integration of the intensity of reflections and scaling, SADABS[18b] for absorption correction, and SHELXTL[18c,18d] for space group and structure determination and least-squares refinements on F^2. All the structures were solved by direct methods using the program SHELXS-97[18e] and refined by full-matrix least-squares methods against F^2 with SHELXL-97.[18e] Hydrogen atoms were fixed at calculated positions, and their positions were refined by a riding model. All non-hydrogen atoms were refined with anisotropic displacement parameters. The disordered water molecules were refined isotropically. The crystallographic figures have been generated using the Diamond 3.1e software.[18f]

pBR322 Cleavage Assay. Plasmid cleavage reactions were performed in sodium cacodylate buffer (10 mM, pH 7.5, 32 °C), containing pBR322 (8 ng/μL, Bangalore Genei). A solution of the complexes **2** and **4** (1 mM) in distilled methanol was used for DNA cleavage. Typically, for each cleavage reaction, 16−18 μL of pBR322 supercoiled DNA and 2 μL of the complex-containing solution were used. For scavenger experiments, concentrations used were 100 mM. All cleavage reactions were quenched with 5 μL of loading buffer containing 100 mM of EDTA, 50% glycerol in Tris−HCl, pH 8.0. The samples were loaded on 0.7% agarose gel (Biozym) containing ethidium

Table 1. Crystal and Structure Refinement Parameters for Compounds **2**−**5**

parameters	**2**	**3**	**4**	**5**
formula	$C_{41}H_{48}Cl_2Cu_3N_6O_{16}P_2$	$C_{54}H_{70}Cl_4Cu_4N_{12}O_{10}P_2$	$C_{41}H_{45}Cl_2Cu_3N_9O_{13}P_2$	$C_{108}H_{116}Cl_8Cu_6N_{16}O_{34}P_4$
formula weight	1204.31	1505.12	1195.32	2970.89
temperature	293(2) K	293(2) K	273(2) K	293(2) K
wavelength	0.71069 Å	0.71069 Å	0.71073 Å	0.71073 Å
crystal system	monoclinic	triclinic	monoclinic	triclinic
space group	$P2(1)/n$	$P\bar{1}$	$P2(1)$	$P\bar{1}$
unit cell dimensions				
a, Å	11.277(5)	9.736(5)	9.7651(3)	13.3841(10)
b, Å	21.956(5)	12.313(5)	23.5852(7)	15.5550(11)
c, Å	19.038(5)	14.588(5)	10.5894(3)	18.0727(13)
α, deg	90°	103.858(5)°	90°	67.4790(10)°
β, deg	101.683(5)°	105.855(5)°	100.883(2)°	72.6560(10)°
γ, deg	90°	95.954(5)°	90°	68.8420(10)°
volume (Å^3), Z	4616(3), 4	1606.3(12), 1	2395.00(12), 2	3185.0(4), 1
d_c /M gm^{-3}	1.733	1.556	1.658	1.549
abs. coef. mm^{-1}	1.634	1.586	1.571	1.283
F(000)	2460	772	1218	1518
crystal size (mm)	0.14 × 0.10 × 0.08	0.17 × 0.10 × 0.07	0.15 × 0.09 × 0.08	0.15 × 0.10 × 0.07
θ range /deg	2.06 to 26.00°	1.95 to 26.00°	1.73 to 26.00°	2.20 to 26.00°
limiting indices	$-13 \le h \le 0$, $-27 \le k \le 20$, $-21 \le l \le 23$	$-6 \le h \le 12$, $-15 \le k \le 15$, $-17 \le l \le 16$	$-10 \le h \le 12$, $-29 \le k \le 24$, $-12 \le l \le 13$	$-16 \le h \le 14$, $-19 \le k \le 18$, $-22 \le l \le 14$
reflections collected	25937	9128	24350	18082
reflections unique [R_{int}]	9068 [0.0553]	6173 [0.0506]	8427 [0.0754]	12289 [0.0437]
completeness to θ	99.9% (θ = 26.00)	97.8% (θ = 26.00)	99.9% (θ = 26.00)	98.0% (θ = 26.00)
data/ restraints/ parameters	9068/0/641	6173/0/396	8427/1/662	12289/242/875
GoF on F^2	1.055	1.016	1.012	1.030
final R indices [$I > 2\sigma(I)$]	R1 = 0.0492, wR2 = 0.1140	R1 = 0.0751, wR2 = 0.1802	R1 = 0.0462, wR2 = 0.1292	R1 = 0.0842, wR2 = 0.2262
R indices (all data)	R1 = 0.0665, wR2 = 0.1215	R1 = 0.1196, wR2 = 0.2142	R1 = 0.0536, R2 = 0.1395	R1 = 0.1345, wR2 = 0.2666
Largest residual peaks/e Å^{-3}	1.390, −0.957	0.771, −0.637	1.822, −0.886	2.386 and −1.300

Table 2. Crystal and Structure Refinement Parameters for Compounds **6**−**8**

parameters	**6**	**7**	**8**
formula	$C_{92}H_{92}Cl_4Cu_6N_{16}O_{39}P_4$	$C_{104}H_{122}Cl_4Cu_6N_{22}O_{36}P_4$	$C_{104}H_{114}Cl_8Cu_6N_{14}O_{34}P_4$
formula weight	2692.74	2903.16	2892.81
temperature	293(2) K	293(2) K	293(2) K
wavelength	0.71069 Å	0.71073 Å	0.71073 Å
crystal system	triclinic	triclinic	triclinic
space group	$P\bar{1}$	$P\bar{1}$	$P\bar{1}$
unit cell dimensions			
a, Å	12.979(5)	13.6524(9)	13.1474(11)
b, Å	18.441(5)	13.7179(9)	14.4528(12)
c, Å	23.548(5)	18.6199(12)	17.3656(15)
α, deg	93.134(5)°	70.4480(10)°	87.873(2)°
β, deg	97.002(5)°	87.0010(10)°	68.8300(10)°
γ, deg	97.235(5)°	65.7410(10)°	71.5580(10)°
volume (Å^3), Z	5535(3), 2	2981.2(3), 1	2907.9(4), 1
d_c /M gm^{-3}	1.616	1.617	1.652
abs. coef. mm^{-1}	1.378	1.285	1.403
F(000)	2740	1490	1478
crystal size (mm)	0.10 × 0.06 × 0.05	0.15 × 0.10 × 0.07	0.20 × 0.15 × 0.08
θ range /deg	2.07 to 26.00°.	2.11 to 25.00°	2.49 to 26.00°
limiting indices	$-14 \le h \le 16$, $-22 \le k \le 21$, $-20 \le l \le 29$	$-16 \le h \le 10$, $-16 \le k \le 15$, $-22 \le l \le 22$	$-16 \le h \le 15$, $-17 < k \le 15$, $-21 < l \le 17$
reflections collected	31544	15671	16213
independent reflections [R_{int}]	21350 [0.0717]	10384 [0.0300]	11160 [0.0268]
completeness to θ	98.2% (θ = 26.00)	98.7% (θ = 25.00)	97.6% (θ = 26.00)
data/ restraints/ parameters	21350/92/1471	10384/0/809	11160/1/822
GooF on F^2	0.949	1.043	1.058
final R indices [$I > 2\sigma(I)$]	R1 = 0.0841, wR2 = 0.1902	R1 = 0.0687, wR2 = 0.1698	R1 = 0.0711, wR2 = 0.1980
R indices (all data)	R1 = 0.1621, wR2 = 0.2464	R1 = 0.0817, wR2 = 0.1805	R1 = 0.0925, wR2 = 0.2220
largest residual peaks/e Å^{-3}	1.401, −0.797	2.581 and −1.800	2.001 and −1.798

bromide (1 μg/1 mL). Electrophoresis was done for 1 h at constant current (80 mA) in 0.5 X TBE buffer. Gels were imaged with a PC-interfaced Bio-Rad Gel Documentation System 2000.

Plasmid Cleavage under Anaerobic Conditions. Oxygen-free nitrogen was bubbled through cacodylate buffer, which was then subjected to four freeze−thaw cycles. All reagents were

Scheme 1

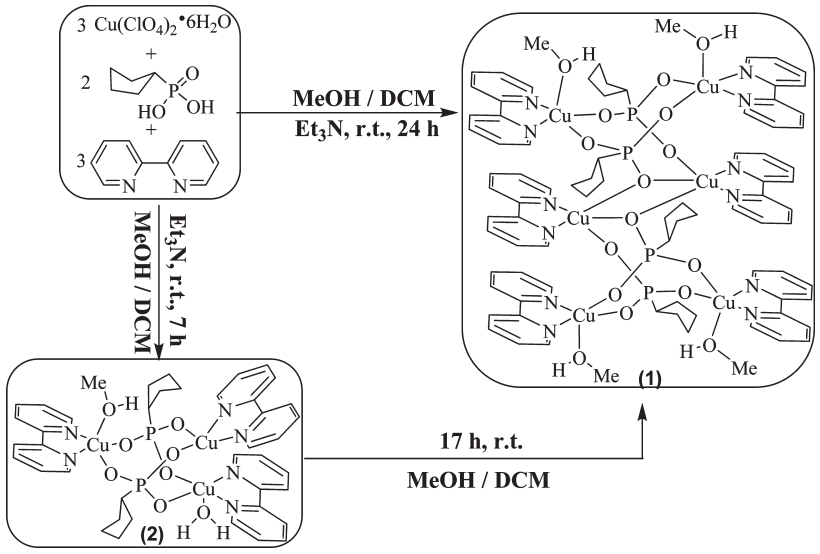

transferred in an argon filled glovebag and eppendorf tubes were tightly sealed with parafilm in the argon atmosphere. Reactions were quenched with loading buffer and efforts were made to ensure strict anaerobic conditions during irradiation and quenching.

Results and Discussion

Synthetic Aspects. A three component reaction involving $Cu(ClO_4)_2 \cdot 6H_2O$, cyclopentyl phosphonic acid, and 2,2′-bipyridine in the presence of triethylamine afforded the trinuclear compound $[Cu_3(C_5H_9PO_3)_2(bpy)_3(MeOH)(H_2O)](ClO_4)_2$ (**2**) (Scheme 1). Continuation of the reaction for prolonged periods (~24 h) leads to the isolation of a hexanuclear derivative $[Cu_6(C_5H_9PO_3)_4(bpy)_6(MeOH)_4](ClO_4)_4$ (**1**) (Scheme 1). The synthesis and characterization of **1** has been previously reported.[15] Thus, **2** represents an intermediate species that dimerizes upon continuation of the reaction. Using $CuCl_2$ instead of $Cu(ClO_4)_2 \cdot 6H_2O$ in the above reaction does not allow the reaction to proceed via the trinuclear derivative **2**. Instead, a tetranuclear complex, containing two $[Cu_2OCl]$ units, $[Cu_4(C_5H_9PO_3)_2(\mu\text{-}Cl)_2(bpya)_4](Cl)_2$ (**3**), is obtained (Scheme 2). The latter can be transformed into a trinuclear derivative. Thus, an in situ generated **3** reacts with $NaClO_4$ to afford the trinuclear complex $[Cu_3(C_5H_9PO_3)_2(\mu\text{-}Cl)(bpya)_3(H_2O)](ClO_4)$ (**4**) (Scheme 2). We have explored the possibility of bridging two trinuclear motifs with appropriate bridging ligands. Accordingly double and single-bridged hexanuclear species, $[\{Cu_3(C_5H_9PO_3)_2(bpy)_3(bpp)\}(MeOH)_2(H_2O)(CH_2Cl_2)(ClO_4)_2]_2$ (**5**), $[\{Cu_3(i\text{-}PrPO_3)_2(bpy)_3(4,4'\text{-}bpy)(H_2O)\}(H_2O)_2(ClO_4)_2]_2$ (**6**), $[\{Cu_3(C_5H_9PO_3)_2(bpya)_3(4,4'\text{-}bpy)(H_2O)\}(MeOH)(H_2O)(ClO_4)_2]_2$ (**7**), and $[Cu_6(t\text{-}BuPO_3)_4(phen)_6(4,4'\text{-}bpy)(MeOH)_4](CH_2Cl_2)(H_2O)(ClO_4)_4$ (**8**), were isolated by the reaction of an in situ generated trinuclear complex with appropriate bridging ligands (Scheme 3). The electronic spectra of **2**−**8** reveal a broad d-d transition in the region of 670 ± 15 nm (see Experimental Section). ESI-MS spectra of the trinuclear derivatives **2** and **4** reveal that they retain their structures in solution as indicated by the presence of peaks at m/z = 478.5 corresponding to $[Cu_3(C_5H_9PO_3)_2(bpy)_3]^{2+}$ for **2**

Scheme 2

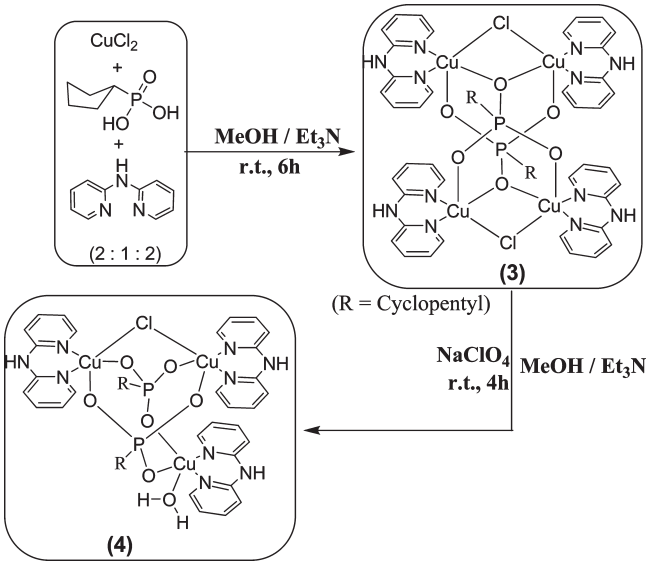

(Figure S1, Supporting Information) and at 1054.0 corresponding to $[Cu_3(C_5H_9PO_3)_2(\mu\text{-}Cl)(bpya)_3(H_2O)]^+$ for **4** (Figure S3, Supporting Information). Similarly the tetranuclear derivative **3** (Figure S2, Supporting Information) also retains its integrity in solution based on the ESI-MS experiments. A peak at m/z = 653.007 was found for **3** and corresponds to $[Cu_4(C_5H_9PO_3)_2(\mu\text{-}Cl)_2(bpya)_4]^{2+}$. In contrast to the behavior of **2**−**4** the bridged hexanuclear complexes **5**−**8** appear to fall apart in solution, and peaks due to the trinuclear unit (and other fragments) could be observed (Supporting Information).

X-ray Crystallography. Bond angle and bond distance data for compounds **2**−**8** are given in Tables 3−9. The molecular structures of these compounds are discussed below.

Molecular Structures of the Trinuclear Compounds 2 and 4. The molecular structures of **2** and **4** are shown in Figures 1 and 2. Compounds **2** and **4** are di- and monocationic complexes respectively. The perchlorate counteranions are non-coordinating. The molecular structures of

Scheme 3

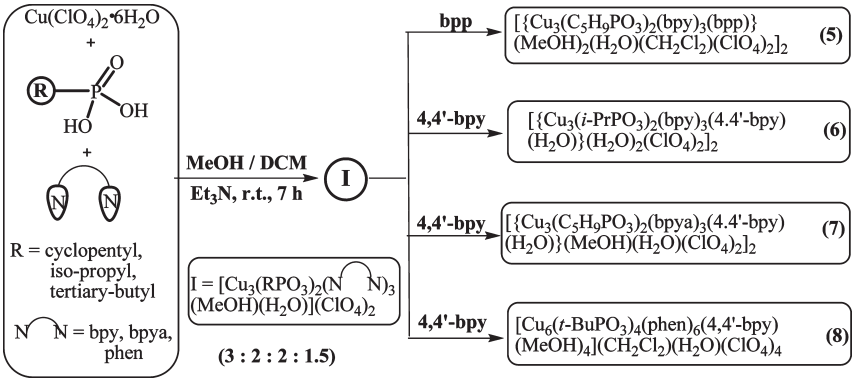

Table 3. Bond Lengths [Å] and Angles [deg] for **2**[a]

Bond Lengths/Å or Bond Angles/deg		
Cu(1)−O(1) 1.922(3)	Cu(2)−O(5) 1.889(3)	Cu(3)−N(6) 2.017(3)
Cu(1)−O(4) 1.924(3)	Cu(2)−N(3) 1.990(3)	Cu(3)−O(8) 2.248(3)
Cu(1)−N(1) 2.020(3)	Cu(2)−N(4) 1.993(3)	P(1)−O(1) 1.520(3)
Cu(1)−N(2) 2.022(3)	Cu(3)−O(6) 1.933(3)	P(1)−O(3) 1.527(3)
Cu(1)−O(7) 2.315(3)	Cu(3)−O(3) 1.947(3)	P(1)−O(2) 1.542(3)
Cu(2)−O(2) 1.888(3)	Cu(3)−N(5) 2.014(3)	
O(1)−Cu(1)−O(4) 100.27(11)	N(2)−Cu(1)−O(7) 100.12(12)	O(3)−Cu(3)−N(5) 155.27(12)
O(1)−Cu(1)−N(1) 89.48(12)	O(2)−Cu(2)−O(5) 98.01(12)	O(6)−Cu(3)−N(6) 171.87(12)
O(4)−Cu(1)−N(1) 165.09(12)	O(2)−Cu(2)−N(3) 169.63(13)	O(3)−Cu(3)−N(6) 91.53(12)
O(1)−Cu(1)−N(2) 166.80(13)	O(5)−Cu(2)−N(3) 90.60(12)	N(5)−Cu(3)−N(6) 80.28(12)
O(4)−Cu(1)−N(2) 88.72(12)	O(2)−Cu(2)−N(4) 91.75(12)	O(6)−Cu(3)−O(8) 92.38(12)
N(1)−Cu(1)−N(2) 79.91(13)	O(5)−Cu(2)−N(4) 165.88(13)	O(3)−Cu(3)−O(8) 99.10(11)
O(1)−Cu(1)−O(7) 89.51(11)	N(3)−Cu(2)−N(4) 80.88(13)	N(5)−Cu(3)−O(8) 104.03(12)
O(4)−Cu(1)−O(7) 90.62(12)	O(6)−Cu(3)−O(3) 96.09(11)	N(6)−Cu(3)−O(8) 89.19(12)
N(1)−Cu(1)−O(7) 100.80(13)	O(6)−Cu(3)−N(5) 91.60(12)	

[a]Symmetry transformations used to generate equivalent atoms: * $-x + 1$, $-y + 2$, $-z$.

2 and **4** are very similar and contain a tricopper ensemble held together by two capping tridentate $[RPO_3]^{2-}$ ligands (3.111 mode[19] of coordination). This coordination mode leads to the generation a bicyclic ring in **2** which contains two eight-membered $Cu_2P_2O_4$ rings. Of the three copper atoms present in **2**, Cu1 and Cu3 are pentacoordinate (2N, 3O) and display a distorted square pyramidal geometry (Supporting Information). The apical positions in these copper atoms are occupied by solvent methanol and water molecules, respectively. Cu2 is tetracoordinate

Table 4. Bond Lengths [Å] and Angles [deg] for **3**

Bond Lengths/Å or Bond Angles/deg		
Cu(1)−O(3) 1.949(5)	Cu(1)−Cl(1) 2.617(2)	Cu(2)−O(1) 2.100(4)
Cu(1)−N(1) 1.999(6)	Cu(2)−O(2) 1.917(5)	Cu(2)−Cl(1) 2.615(2)
Cu(1)−N(3) 2.008(6)	Cu(2)−N(4) 2.008(6)	P(1)−O(2) 1.518(5)
Cu(1)−O(1) 2.014(4)	Cu(2)−N(6) 2.036(5)	P(1)−O(3) 1.518(5)
O(3)−Cu(1)−N(1) 84.9(2)	N(1)−Cu(1)−Cl(1) 103.82(19)	N(4)−Cu(2)−O(1) 92.3(2)
O(3)−Cu(1)−N(3) 161.4(2)	N(3)−Cu(1)−Cl(1) 104.62(18)	N(6)−Cu(2)−O(1) 153.8(2)
N(1)−Cu(1)−N(3) 88.7(2)	O(1)−Cu(1)−Cl(1) 81.90(13)	O(2)−Cu(2)−Cl(1) 92.96(16)
O(3)−Cu(1)−O(1) 94.26(18)	O(2)−Cu(2)−N(4) 170.6(2)	N(4)−Cu(2)−Cl(1) 96.10(18)
N(1)−Cu(1)−O(1) 174.2(2)	O(2)−Cu(2)−N(6) 85.1(2)	N(6)−Cu(2)−Cl(1) 125.68(18)
N(3)−Cu(1)−O(1) 90.4(2)	N(4)−Cu(2)−N(6) 87.5(2)	O(1)−Cu(2)−Cl(1) 80.41(13)
O(3)−Cu(1)−Cl(1) 93.85(15)	O(2)−Cu(2)−O(1) 91.79(19)	Cu(2)−Cl(1)−Cu(1) 79.33(6)

Table 5. Bond Lengths [Å] and Angles [deg] for **4**

Bond Lengths/Å or Bond Angles/deg		
Cu(1)−O(1) 1.916(4)	Cu(2)−O(2) 1.972(4)	Cu(3)−N(7) 2.005(5)
Cu(1)−N(1) 1.987(5)	Cu(2)−N(4) 1.990(5)	Cu(3)−N(8) 2.007(5)
Cu(1)−O(4) 1.995(4)	Cu(2)−N(6) 2.012(5)	Cu(3)−O(7) 2.343(5)
Cu(1)−N(2) 2.018(5)	Cu(2)−Cl(1) 2.7009(15)	P(1)−O(1) 1.505(4)
Cu(1)−Cl(1) 2.5733(14)	Cu(3)−O(6) 1.931(4)	P(1)−O(3) 1.525(4)
Cu(2)−O(5) 1.901(4)	Cu(3)−O(3) 1.936(4)	P(1)−O(2) 1.533(4)
O(1)−Cu(1)−N(1) 164.60(18)	O(5)−Cu(2)−N(4) 170.73(18)	O(6)−Cu(3)−N(7) 89.30(18)
O(1)−Cu(1)−O(4) 93.24(17)	O(2)−Cu(2)−N(4) 87.59(18)	O(3)−Cu(3)−N(7) 171.25(19)
N(1)−Cu(1)−O(4) 89.20(18)	O(5)−Cu(2)−N(6) 87.66(18)	O(6)−Cu(3)−N(8) 171.66(17)
O(1)−Cu(1)−N(2) 86.10(19)	O(2)−Cu(2)−N(6) 158.46(19)	O(3)−Cu(3)−N(8) 90.07(17)
N(1)−Cu(1)−N(2) 85.8(2)	N(4)−Cu(2)−N(6) 87.23(19)	N(7)−Cu(3)−N(8) 87.47(19)
O(4)−Cu(1)−N(2) 157.09(18)	O(5)−Cu(2)−Cl(1) 88.96(13)	O(6)−Cu(3)−O(7) 92.82(17)
O(1)−Cu(1)−Cl(1) 95.78(13)	O(2)−Cu(2)−Cl(1) 107.85(12)	O(3)−Cu(3)−O(7) 93.90(18)
N(1)−Cu(1)−Cl(1) 98.20(14)	N(4)−Cu(2)−Cl(1) 99.07(14)	N(7)−Cu(3)−O(7) 94.7(2)
O(4)−Cu(1)−Cl(1) 105.63(12)	N(6)−Cu(2)−Cl(1) 93.61(16)	N(8)−Cu(3)−O(7) 95.11(18)
N(2)−Cu(1)−Cl(1) 97.21(14)	O(6)−Cu(3)−O(3) 91.98(16)	Cu(1)−Cl(1)−Cu(2) 92.13(5)
O(5)−Cu(2)−O(2) 94.36(17)		

(18) (a) *SMART & SAINT Software Reference manuals*, Version 6.45; Bruker Analytical X-ray Systems, Inc.: Madison, WI, 2003. (b) Sheldrick, G. M. SADABS, a software for empirical absorption correction, Ver. 2.05; University of Göettingen: Göettingen, Germany, 2002. (c) SHELXTL Reference Manual, Ver. 6.c1; Bruker Analytical X-ray Systems, Inc.: Madison, WI, 2000. (d) Sheldrick, G. M. SHELXTL, Ver. 6.12; Bruker AXS Inc.: Madison, WI, 2001. (e) Sheldrick, G. M. SHELXL97, Program for Crystal Structure Refinement; University of Geöttingen: Göettingen, Germany, 1997. (f) Bradenburg, K. Diamond, Ver. 3.1eM; Crystal Impact GbR: Bonn, Germany, 2005.

(19) Coxall, R. A.; Harris, S. G.; Henderson, S.; Parsons, S.; Taskar, R. A.; Winpenny, R. E. P. *J. Chem. Soc., Dalton Trans*. **2000**, *14*, 2349.

Table 6. Bond Lengths [Å] and Angles [deg] for **5**[a]

Bond Lengths/Å or Bond Angles/deg		
Cu(1)−O(1) 1.888(5)	Cu(2)−N(3) 2.037(6)	P(1)−O(1) 1.517(5)
Cu(1)−O(6) 1.894(5)	Cu(2)−N(7) 2.216(7)	P(1)−O(2) 1.528(5)
Cu(1)−N(2) 1.999(7)	Cu(3)−O(3) 1.932(5)	P(1)−O(3) 1.529(5)
Cu(1)−N(1) 2.019(6)	Cu(3)−O(5) 1.942(5)	P(2)−O(5) 1.516(5)
Cu(2)−O(2) 1.927(5)	Cu(3)−N(5) 2.017(7)	P(2)−O(6) 1.523(5)
Cu(2)−O(4) 1.939(5)	Cu(3)−N(6) 2.028(6)	P(2)−O(4) 1.528(5)
Cu(2)−N(4) 2.014(6)	Cu(3)−N(8) 2.265(7)	
O(1)−Cu(1)−O(6) 100.7(2)	O(2)−Cu(2)−N(3) 90.6(2)	O(5)−Cu(3)−N(5) 167.8(2)
O(1)−Cu(1)−N(2) 169.3(2)	O(4)−Cu(2)−N(3) 156.2(2)	O(3)−Cu(3)−N(6) 163.8(3)
O(6)−Cu(1)−N(2) 89.7(2)	N(4)−Cu(2)−N(3) 79.7(3)	O(5)−Cu(3)−N(6) 91.0(2)
O(1)−Cu(1)−N(1) 89.9(2)	O(2)−Cu(2)−N(7) 99.2(2)	N(5)−Cu(3)−N(6) 79.8(3)
O(6)−Cu(1)−N(1) 169.3(2)	O(4)−Cu(2)−N(7) 106.0(2)	O(3)−Cu(3)−N(8) 94.2(2)
N(2)−Cu(1)−N(1) 79.7(3)	N(4)−Cu(2)−N(7) 94.1(2)	O(5)−Cu(3)−N(8) 91.3(2)
O(2)−Cu(2)−O(4) 94.6(2)	N(3)−Cu(2)−N(7) 96.0(2)	N(5)−Cu(3)−N(8) 98.1(3)
O(2)−Cu(2)−N(4) 164.3(2)	O(3)−Cu(3)−O(5) 96.8(2)	N(6)−Cu(3)−N(8) 99.7(2)
O(4)−Cu(2)−N(4) 89.7(2)	O(3)−Cu(3)−N(5) 90.2(2)	

[a] Symmetry transformations used to generate equivalent atoms: * $-x$, $-y$, $-z+1$.

Table 7. Bond Lengths [Å] and Angles [deg] for **6**[a]

Bond Lengths/Å or Bond Angles/deg		
Cu(1)−O(2) 1.943(6)	Cu(3)−N(5) 2.023(7)	Cu(5)−N(15) 2.241(7)
Cu(1)−O(6) 1.950(6)	Cu(3)−N(6) 2.058(7)	Cu(6)−O(9) 1.918(5)
Cu(1)−N(2) 2.008(7)	Cu(3)−N(13) 2.233(7)	Cu(6)−O(11) 1.945(6)
Cu(1)−N(1) 2.033(7)	Cu(4)−O(7) 1.934(6)	Cu(6)−N(11) 2.009(7)
Cu(1)−O(29) 2.231(6)	Cu(4)−O(10) 1.940(6)	Cu(6)−N(12) 2.062(7)
Cu(2)−O(1) 1.908(6)	Cu(4)−N(7) 1.994(7)	Cu(6)−N(16)* 2.242(7)
Cu(2)−O(5) 1.936(6)	Cu(4)−N(8) 2.043(7)	P(1)−O(3) 1.515(6)
Cu(2)−N(4) 2.026(7)	Cu(4)−O(30) 2.240(6)	P(1)−O(1) 1.525(7)
Cu(2)−N(3) 2.059(7)	Cu(5)−O(12) 1.918(6)	P(1)−O(2) 1.560(7)
Cu(2)−N(14)* 2.241(7)	Cu(5)−O(8) 1.933(6)	P(2)−O(5) 1.516(6)
Cu(3)−O(3) 1.919(6)	Cu(5)−N(9) 2.025(7)	P(2)−O(4) 1.519(6)
Cu(3)−O(4) 1.932(6)	Cu(5)−N(10) 2.032(7)	P(2)−O(6) 1.534(6)
O(2)−Cu(1)−O(6) 94.6(2)	O(1)−Cu(2)−O(5) 97.3(3)	O(3)−Cu(3)−O(4) 98.9(2)
O(2)−Cu(1)−N(2) 173.3(3)	O(1)−Cu(2)−N(4) 163.7(3)	O(3)−Cu(3)−N(5) 90.8(3)
O(6)−Cu(1)−N(2) 91.5(3)	O(5)−Cu(2)−N(4) 90.4(3)	O(4)−Cu(3)−N(5) 166.5(3)
O(2)−Cu(1)−N(1) 93.8(3)	O(1)−Cu(2)−N(3) 91.0(3)	O(3)−Cu(3)−N(6) 160.1(3)
O(6)−Cu(1)−N(1) 161.4(3)	O(5)−Cu(2)−N(3) 167.1(3)	O(4)−Cu(3)−N(6) 88.7(3)
N(2)−Cu(1)−N(1) 79.6(3)	N(4)−Cu(2)−N(3) 79.2(3)	N(5)−Cu(3)−N(6) 79.2(3)
O(2)−Cu(1)−O(29) 88.4(3)	O(1)−Cu(2)−N(14)* 98.4(3)	O(3)−Cu(3)−N(13) 101.2(2)
O(6)−Cu(1)−O(29) 105.8(3)	O(5)−Cu(2)−N(14)* 96.2(3)	O(4)−Cu(3)−N(13) 93.8(3)
N(2)−Cu(1)−O(29) 92.6(3)	N(4)−Cu(2)−N(14)* 95.0(3)	N(5)−Cu(3)−N(13) 93.5(3)
N(1)−Cu(1)−O(29) 91.0(3)	N(3)−Cu(2)−N(14)* 92.4(3)	N(6)−Cu(3)−N(13) 96.6(3)

[a] Symmetry transformations used to generate equivalent atoms: * $-x$, $-y$, $-z+1$ * $-x+1$, $-y+1$, $-z+2$.

(2N, 2O) in a distorted square planar geometry. All the three copper atoms contain a chelating bipyridyl ring. The molecular structure of **4** is only slightly different from

Table 8. Bond Lengths [Å] and Angles [deg] for **7**[a]

Bond Lengths/Å or Bond Angles/deg		
Cu(1)−O(4) 1.928(4)	Cu(2)−N(4) 2.024(4)	N(11)−Cu(2)* 2.296(5)
Cu(1)−O(1) 1.931(4)	Cu(2)−N(11)* 2.296(5)	P(1)−O(1) 1.525(4)
Cu(1)−N(1) 2.015(4)	Cu(3)−O(3) 1.888(4)	P(1)−O(3) 1.526(4)
Cu(1)−N(3) 2.050(4)	Cu(3)−N(7) 1.979(5)	P(1)−O(2) 1.528(4)
Cu(1)−N(10) 2.252(4)	Cu(3)−O(6) 1.994(4)	P(2)−O(5) 1.520(4)
Cu(2)−O(5) 1.932(4)	Cu(3)−N(9) 2.047(5)	P(2)−O(4) 1.521(4)
Cu(2)−O(2) 1.934(4)	Cu(3)−O(7) 2.301(4)	P(2)−O(6) 1.549(4)
Cu(2)−N(6) 2.012(5)		
O(4)−Cu(1)−O(1) 95.10(15)	O(5)−Cu(2)−O(2) 94.66(15)	O(3)−Cu(3)−N(7) 171.97(19)
O(4)−Cu(1)−N(1) 173.23(17)	O(5)−Cu(2)−N(6) 172.1(2)	O(3)−Cu(3)−O(6) 97.88(15)
O(1)−Cu(1)−N(1) 86.34(17)	O(2)−Cu(2)−N(6) 87.62(18)	N(7)−Cu(3)−O(6) 87.68(17)
O(4)−Cu(1)−N(3) 89.80(16)	O(5)−Cu(2)−N(4) 89.22(17)	O(3)−Cu(3)−N(9) 91.10(17)
O(1)−Cu(1)−N(3) 158.71(17)	O(2)−Cu(2)−N(4) 167.28(17)	N(7)−Cu(3)−N(9) 88.3(2)
N(1)−Cu(1)−N(3) 86.54(18)	N(6)−Cu(2)−N(4) 87.0(2)	O(6)−Cu(3)−N(9) 139.73(16)
O(4)−Cu(1)−N(10) 90.71(16)	O(5)−Cu(2)−N(11)* 94.09(16)	O(3)−Cu(3)−O(7) 83.94(16)
O(1)−Cu(1)−N(10) 98.45(16)	O(2)−Cu(2)−N(11)* 97.68(16)	N(7)−Cu(3)−O(7) 88.21(19)
N(1)−Cu(1)−N(10) 95.63(17)	N(6)−Cu(2)−N(11)* 93.1(2)	O(6)−Cu(3)−O(7) 121.72(15)
N(3)−Cu(1)−N(10) 102.19(17)	N(4)−Cu(2)−N(11)* 94.11(17)	N(9)−Cu(3)−O(7) 98.16(17)

[a] Symmetry transformations used to generate equivalent atoms: * $-x+1$, $-y+1$,$-z$.

Table 9. Bond Lengths [Å] and Angles [deg] for **8**[a]

Bond Lengths/Å or Bond Angles/deg		
Cu(1)−O(5) 1.901(4)	Cu(2)−N(4) 2.018(5)	Cu(3)−N(7) 2.264(4)
Cu(1)−O(3) 1.927(4)	Cu(2)−N(3) 2.027(5)	P(1)−O(1) 1.524(4)
Cu(1)−N(1) 2.024(5)	Cu(2)−O(15) 2.408(6)	P(1)−O(2) 1.531(4)
Cu(1)−N(2) 2.037(5)	Cu(3)−O(1) 1.910(4)	P(1)−O(3) 1.531(4)
Cu(1)−O(16) 2.303(4)	Cu(3)−O(6) 1.952(4)	P(2)−O(4) 1.525(4)
Cu(2)−O(2) 1.893(4)	Cu(3)−N(6) 2.033(5)	P(2)−O(5) 1.530(4)
Cu(2)−O(4) 1.931(4)	Cu(3)−N(5) 2.051(4)	P(2)−O(6) 1.538(4)
O(5)−Cu(1)−O(3) 98.60(16)	O(2)−Cu(2)−O(4) 99.25(16)	O(1)−Cu(3)−O(6) 98.64(16)
O(5)−Cu(1)−N(1) 166.78(18)	O(2)−Cu(2)−N(4) 170.60(17)	O(1)−Cu(3)−N(6) 165.76(17)
O(3)−Cu(1)−N(1) 91.36(18)	O(4)−Cu(2)−N(4) 90.14(17)	O(6)−Cu(3)−N(6) 91.03(17)
O(5)−Cu(1)−N(2) 88.81(19)	O(2)−Cu(2)−N(3) 89.50(17)	O(1)−Cu(3)−N(5) 88.48(18)
O(3)−Cu(1)−N(2) 169.31(19)	O(4)−Cu(2)−N(3) 169.28(18)	O(6)−Cu(3)−N(5) 167.61(17)
N(1)−Cu(1)−N(2) 80.2(2)	N(4)−Cu(2)−N(3) 81.20(19)	N(6)−Cu(3)−N(5) 80.3(2)
O(5)−Cu(1)−O(16) 90.52(16)	O(2)−Cu(2)−O(15) 90.21(18)	O(1)−Cu(3)−N(7) 93.21(17)
O(3)−Cu(1)−O(16) 92.57(17)	O(4)−Cu(2)−O(15) 90.3(2)	O(6)−Cu(3)−N(7) 103.30(16)
N(1)−Cu(1)−O(16) 97.73(17)	N(4)−Cu(2)−O(15) 89.37(19)	N(6)−Cu(3)−N(7) 94.71(17)
N(2)−Cu(1)−O(16) 95.08(18)	N(3)−Cu(2)−O(15) 95.9(2)	N(5)−Cu(3)−N(7) 86.30(17)

[a] Symmetry transformations used to generate equivalent atoms: * $-x+1$, $-y$, $-z$.

that of **2**. Copper atoms Cu1 and Cu2 are further bridged in this case by a chloride ligand. As a result all the copper atoms in **4** are five-coordinate in a distorted square pyramidal geometry (Supporting Information, Table S1).

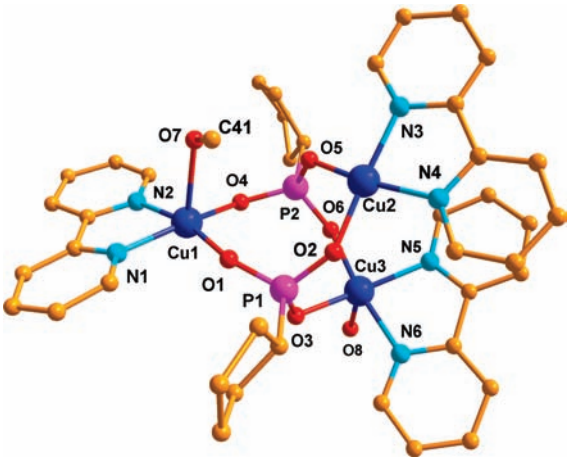

Figure 1. View of the trinuclear cation part of **2.** Perchlorate anions and hydrogen atoms have been removed for the sake of clarity.

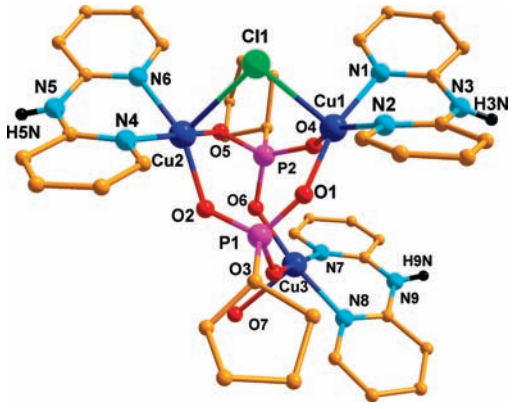

Figure 2. View of the trinuclear cation part of **4.** Perchlorate anions and hydrogen atoms have been removed for the sake of clarity.

Among the Cu−O bond distances, those involving the phosphonate ligand are shorter (1.888 (3) Å in **2** and 1.901(4) Å in **4**) in comparison to those involving the solvent molecules [Cu1−O7: 2.315(3) Å; Cu3−O8: 2.248 (3) Å in **2**. Cu3−O7: 2.343(5) Å in **4**]. The average P−O bond distance in **2** is 1.530 (3) Å while in **4** it is 1.521 (4) Å. In **2** the Cu−N distances involving the chelating bipyridine ligands are nearly similar (average Cu−N: 2.006(3) Å). In **4** also the various Cu−N distances are nearly similar to each other (average Cu−N: 1.992 (5) Å) and are comparable to that observed in **2**. It is interesting to compare the bond parameters observed in these trinuclear compounds with $[Cu_3(Me_3tacn)_3(PhOPO_3)_2](ClO_4)_2 \cdot 1/2H_2O$ [Me_3tacn (1,4,7-trimethyl-1,4,7-triazacyclononane)].[20] The Cu−O distances involving the monophosphate ester ligands are 1.917 (2) and 1. 932 (2) Å while the Cu−N distances are 2.073 (2) and 2.057 (2) Å, respectively. These distances are comparable to those found in the present instance.

Molecular Structure of the Tetranuclear Complex 3. The molecular structure of the tetranuclear complex **3** is shown in Figure 3. It is a dicationic complex with two non-coordinating chloride anions. The four Cu(II) atoms of the tetranuclear assembly are arranged in a rectangular plane.

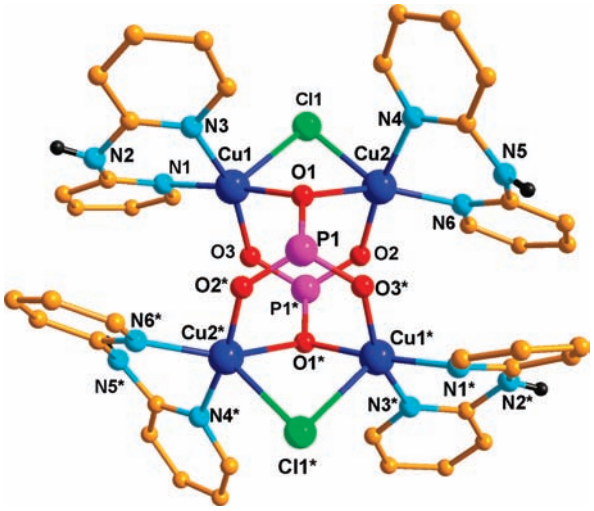

Figure 3. View of the tetranuclear cation part of **3**. Cyclopentyl groups, interstitial chloride anion, solvent molecules and hydrogen atoms have been removed for the sake of clarity.

Two $[RPO_3]^{2-}$ ligands are involved in holding the tetranuclear motif together. Unlike in **2** and **3** the phosphonate ligands are bound to four metal atoms (coordination mode: 4.211). One of the oxygen atoms of each of the phosphonate ligands functions as a bridging ligand (cf. O1 bridges Cu1 and Cu2) while the other two oxygen atoms are monodentate and bind to a copper atom each. In addition to the phosphonate ligands, the two chloride ligands are also involved in maintaining the structural integrity of the core by functioning as bridging ligands to hold two pairs of copper atoms. As a result of this coordination by phosphonate and chloride ligands, the tetranuclear core contains two symmetrically related four-membered Cu_2ClO rings as well as two six-membered Cu_2ClO_2P rings. The four copper atoms in **3** are five-coordinate (2N, 2O, Cl) and display a distorted square-pyramidal geometry (Supporting Information, Table S1) (for bond lengths and angles, see Table 4). The structure of the tetranuclear core of **4** is similar to that found earlier in $[Cu_4(\mu\text{-}Cl)_2(\mu_3\text{-}C_6H_{11}PO_3)_2(bpy)_4](NO_3)_2$ and $[Cu_4(\mu\text{-}CH_3COO)_2(\mu_3\text{-}C_6H_{11}PO_3)_2(bpy)_4]\,(CH_3COO)_2$.[21]

Complex **3** forms a 2D-sheet in its crystal structure as a result of N−H---O, O−H---Cl, N−H---Cl and π---π interactions (Supporting Information). Complexes **2** and **4** also show 2D-supramolecular structures in their solid-state as a result of similar weak interactions (C−H----O, π---π for **2** and N−H---O, O−H---Cl, π---π for **4**) (Supporting Information).

Molecular Structures of the Hexanuclear Assemblies 5−8. The hexanuclear compounds **5−8** are tetracationic complexes and contain four non-coordinating perchlorate anions. The molecular structures of these complexes are given in Figures 4−7. Complexes **5−7** are metallamacrocycles assembled by a pair of linear bridging ligands 1,3-bis(4-pyridyl)propane (bpp) or 4,4′-bipyridine

(20) Fry, F. H.; Jensen, P.; Christopher, M. K.; Leone, S. *Inorg. Chem.* **2003**, *42*, 5367.

(21) (a) Tudo, V.; Kravtsov, V.; Julve, M.; Lloret, F.; Simonov, Y. A.; Lipkowski, J.; Buculei, V.; Andruh, M. *Polyhedron* **2001**, *20*, 3033–3037. (b) Chandrasekhar, V.; Azhakar, R.; Senapati, T.; Thilagar, P.; Ghosh, S.; Verma, S.; Boomishankar, R.; Steiner, A.; Koegerler, P. *Dalton Trans.* **2008**, *9*, 1150.

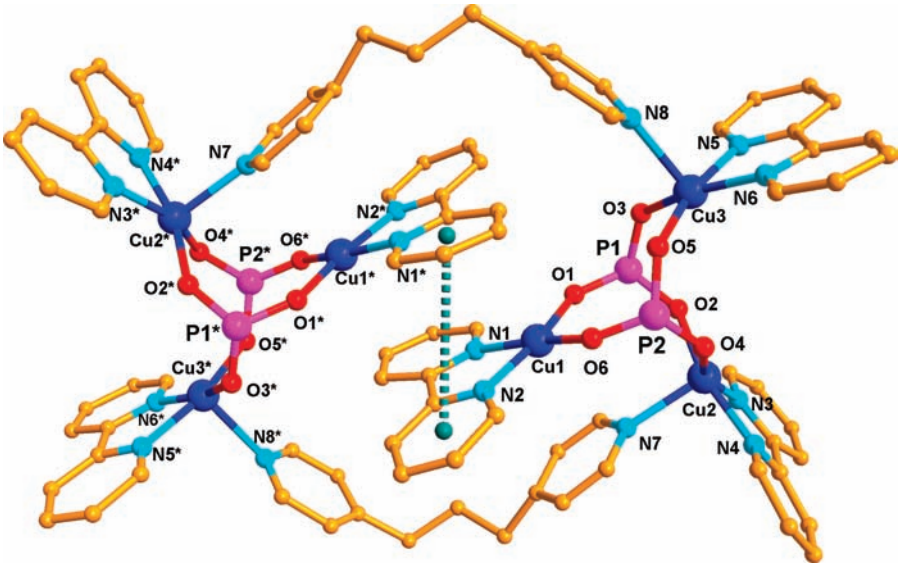

Figure 4. View of the hexanuclear cation part of **5**. Perchlorate anions, interstitial solvent molecules, cyclopentyl groups and hydrogen atoms have been removed for the sake of clarity.

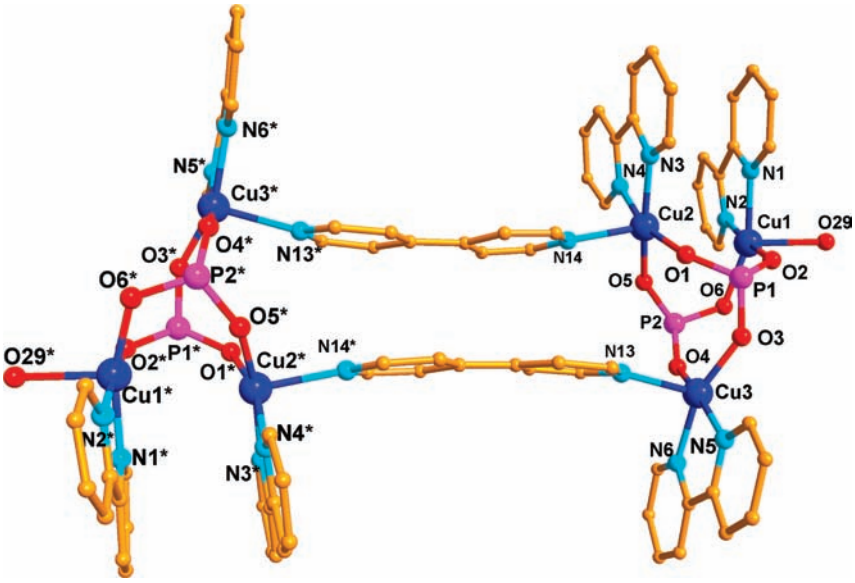

Figure 5. View of the cation part of **6**. Perchlorate anions, interstitial water molecules, isopropyl groups and hydrogen atoms have been removed for the sake of clarity.

(4,4′-bpy). These ligands successfully link two trinuclear copper phosphonate motifs by bridging copper atoms in adjacent trinuclear units. Thus, in **5**, the copper atoms Cu2 and Cu3 are bridged to Cu2* and Cu3*, respectively, to generate a 32-membered macrocycle. The presence of the propyl spacer in the bridging bpp ligand confers a dome-shape to the macrocycle **5**. The relationship of the two trinuclear motifs with respect to each other is *anti*. Within each trinuclear unit while the phosphorus atoms P1 and P2 are perfectly eclipsed; there is a small torsion angle between the corresponding oxygen atoms (O3 and O5; O2 and O4; O1 and O6).

While two of the copper atoms in the trinuclear unit are pentacoordinate the remaining copper atom (Cu1) is tetracoordinate. The two tetracoordinate copper atoms of the hexanuclear unit are located within the macrocyclic dome facilitating a $\pi-\pi$ interaction between the bipyridyl substituents (Figure 4). Among the Cu−O distances those involving Cu1 are shorter (average: 1.891 (5) Å) in comparison to those found with Cu3 and Cu2 (average: 1.936 (5) Å). The former is not involved in coordination by the bridging bpp ligand. Among the Cu−N distances those involving the bpp ligands are slightly longer (average: 2.241 (7) Å) than those found with bpy ligands (average: 2.024 (7) Å).

In contrast to **5**, in **6** and **7** the bridging 4,4′-bpy ligand is more rigid, and its coordination action generates nearly rectangular 26-membered macrocyclic rings. All of the copper atoms in these compounds are five-coordinate. In **6** the two aromatic rings of the 4,4′-bipyridyl ligand are coplanar, but in **7** the aromatic rings of the linker are not coplanar; in fact, the torsion angle between them is 22°. The bond parameters observed in **6** and **7** are comparable to those found in **5 (** Tables 6−8).

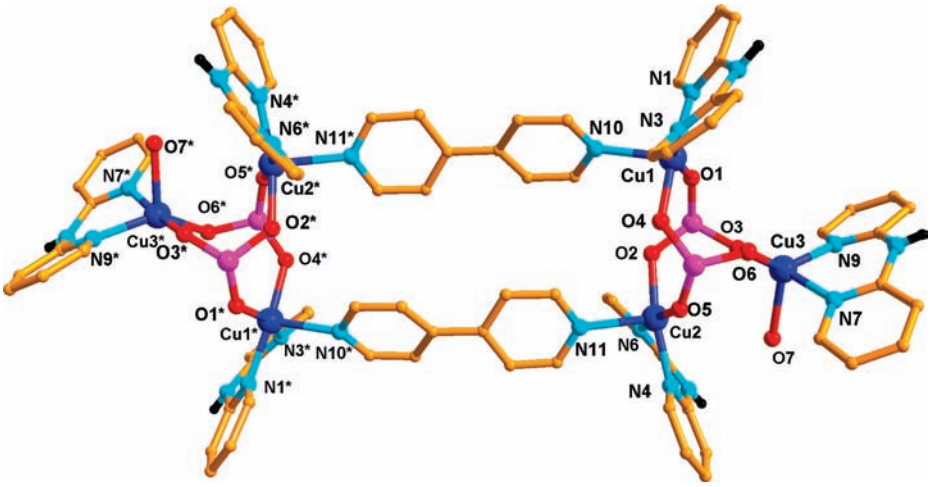

Figure 6. View of the cation part of **7**. Perchlorate anions, interstitial solvent molecules, cyclopentyl groups and hydrogen atoms have been removed for the sake of clarity.

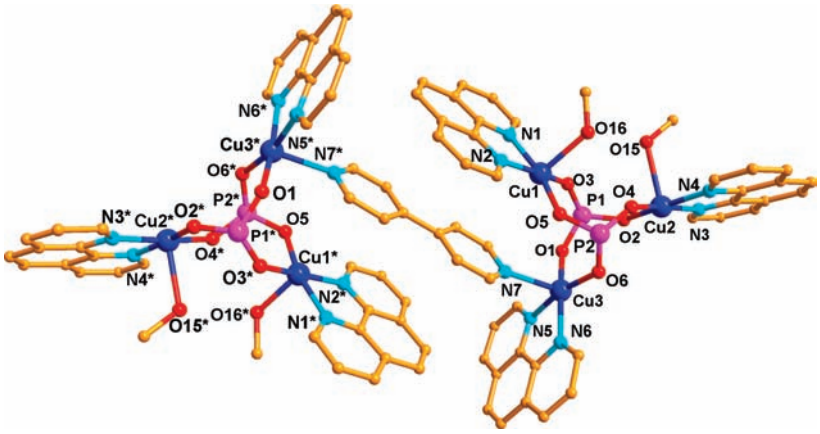

Figure 7. View of the cation part of **8**. Perchlorate anions, interstitial solvent molecules, tertiary butyl groups and hydrogen atoms have been removed for the sake of clarity.

The molecular structure of **8** contains a single linker between the two trinuclear motifs. In this instance the formation of the double bridge is prevented, presumably, by the presence of the more sterically hindered 1,10-phenanthroline ligands on the copper atoms. Also, in **8** the three copper atoms of the trinuclear motifs are five-coordinate; Cu1, Cu2, Cu1*, and Cu2* have a coordinated methanol molecule in their apical positions. Two copper atoms of each trinuclear motif (Cu 1 and Cu 2) contain a methanol molecule in their axial coordination sites. The Cu−O distances involving the coordinated methanol (average: 2.356(6) Å) are longer than those observed with phosphonate ligands (average: 1.913 (4) Å; Table 9).

The structural features of the trinuclear motifs are not distorted by being linked with linear bridging ligands. In fact, the structural features of the trinuclear cores of **5**−**8** are similar to that of complex **2**, discussed earlier. Compounds **5**−**8** do not retain their solid-state structures in solution as evidenced by their ESI-MS data (Supporting Information). Compounds **5**−**7** show supramolecular architectures in the solid-state mediated by C−H---Cu, N−H---O, and π---π interactions (Supporting Information).

Magnetic Studies. Magnetic studies were carried out on the trinuclear and hexanuclear compounds. The magnetic measurements on the tetranuclear derivative were inconclusive because of the presence of magnetic impurities. The latter could not be eliminated in spite of several attempts.

Scheme 4

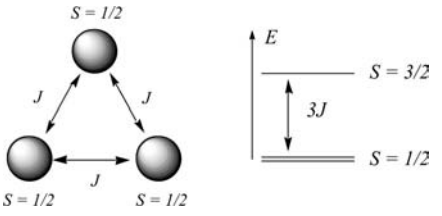

Trinuclear Compounds 2 and 4. At room temperature, the χT products of **2** and **4** are 1.24 and 1.27 cm^3 K mol^{-1}, respectively, in good agreement with the presence of three $S = 1/2$ Cu(II) spins and $g = 2.10$ and 2.12 (note that $S = 1/2$ Cu^{II} metal ions possess a Curie constant of 0.375 cm^3 K mol^{-1} with $g = 2$). Lowering the temperature, the χT product at 1000 Oe continuously decreases to reach 0.40 and 0.42 cm^3 K mol^{-1} at 1.8 K respectively indicating dominant antiferromagnetic interactions in the [Cu_3] complexes.

On the basis of the X-ray crystal structures described above, these complexes can be seen as a first approxima-

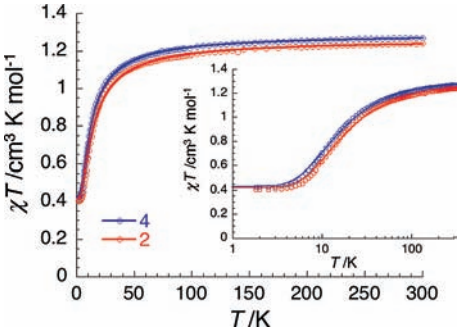

Figure 8. χT vs T plot (with χ being the magnetic susceptibility equal to M/H) for **2** (red), **4** (blue) measured at 1000 Oe. Inset: semilogarithmic χT vs T plot emphasizing the low temperature region. The solid lines are the best fits obtained with the triangular Heisenberg model described in the text.

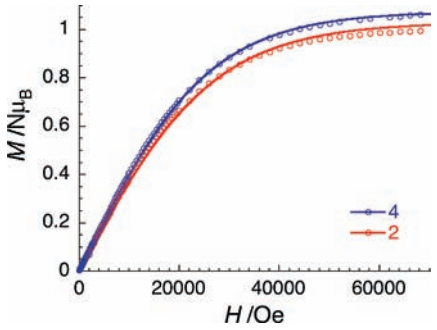

Figure 9. M vs H plot at 1.8 K for **2** (red) and **4** (blue). The solid lines are the best fits obtained with simple $S = 1/2$ Brillouin functions described in the text.

tion as an equilateral triangular system of $S = 1/2$ Cu(II) spins (Scheme 4). The spin Hamiltonian, given in eq 1, can therefore be considered with an isotropic exchange interaction J between spin carriers.

$$H = -2J(S_1 \cdot S_2 + S_2 \cdot S_3 + S_3 \cdot S_1) \qquad (1)$$

This interaction splits the three degenerate energy levels into a quartet state with a total spin $S_T = 3/2$ (where $S_T = S_1 + S_2 + S_3$) and two degenerate doublet ground states with $S_T = 1/2$:

In the low field limit ($k_B T \gg \mu_B H$), the susceptibility derived from the Hamiltonian given in eq 1 can be expressed as eq 2:

$$\chi = \frac{Ng^2\mu_B^2}{4k_B T}\frac{(1 + 5e^{3J/k_B T})}{(1 + e^{3J/k_B T})} \qquad (2)$$

An excellent fit of the experimental data is obtained with the following parameters: $J = -4.4$ (1) cm^{-1} (or $J/k_B = -6.3(1)$ K) and $-3.8(1)$ cm^{-1} (or $J/k_B = -5.5$ (1) K) and $g = 2.12(5)$ and 2.14(5) for **2** and **4**, respectively (Figure 8). It is worth noting that the above model is reproducing extremely well the experimental data and therefore it is impossible to add further parameters such as a second intramolecular magnetic interaction (that is nevertheless present by symmetry in these triangular complexes) without over parametrization. Therefore, it is important to mention that the J value is thus an average value of the intramolecular magnetic interactions. The sign of J is consistent with antiferromagnetic coupling

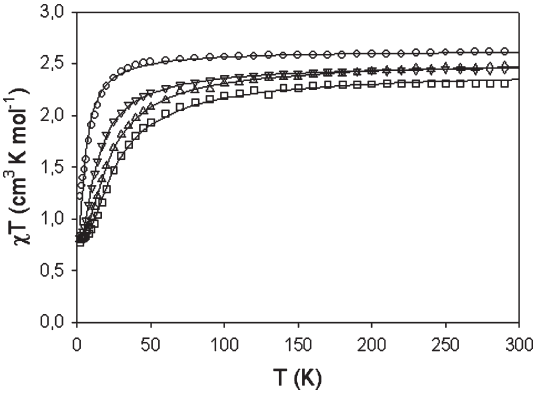

Figure 10. χT vs T plots for **5** (▼), **6** (○), **7** (□), and **8** (Δ) at 500 Oe. The solid lines are the best fit of the experimental data. See text for fitting parameters.

and implies that this trinuclear complex possesses an $S_T = 1/2$ spin ground state in good agreement with the M versus H data at 1.8 K (Figure 9). The magnetization is almost saturated at 7 T to 1.06 and 0.99 μ_B for **2** and **4**, respectively, in agreement with the presence of an $S_T = 1/2$ spin ground state with a g factor close to 2. The M versus H data have been fitted remarkably well to an $S = 1/2$ Brillouin function (Figure 10) confirming a g factor of 2.06(1) and 2.14(1) in very good agreement to the value deduced from the χT versus T data.

Hexanuclear Derivatives 5−8. Variable temperature magnetic susceptibilities were collected for complexes **5**, **6**, **7**, and **8** at 1 T and 500 G applied magnetic fields on crushed crystalline samples. The data are not field dependent and are shown as χT versus T plots in Figure 10. The χT product at 300 K has values between 2.31 and 2.62 cm^3 K mol^{-1}, well in agreement with the expected 2.25 cm^3 K mol^{-1} value for six non-interacting Cu(II) ions with $S = 1/2$ and $g = 2.0$. The χT product slightly decreases with decreasing temperature, until a sharp drop is observed below 50 K, indicating antiferromagnetic coupling between the Cu(II) centers in the complexes. The susceptibility at 2 K has values between 0.77 cm^3 K mol^{-1} and 0.81 cm^3 K mol^{-1} for **5**, **7**, and **8** and 1.22 cm^3 K mol^{-1} for **6**.

The structure of the complexes consists of two [Cu_3] units bridged by one or two organic linkers. Within each trinuclear Cu(II) unit, the magnetic exchange is mediated by two [μ_3-RPO_3]$^{2-}$ groups. All of the Cu(II) ions are pentacoordinated in a distorted square-pyramidal fashion, except in **5** where one Cu(II) on each [Cu_3] unit is tetracoordinated in a square-planar fashion. To model the magnetic data, each hexanuclear complex was considered as two independent [Cu_3] units, and the magnetic data were analyzed using the same equilateral triangular model used for complexes **2** and **4**. The best fittings are shown in Figure 10 as solid lines, and the fitting parameters were $J = -4.14$ cm^{-1} (or $J/k_B = -5.96$ K) and $g = 2.11$ for **5**, $J = -1.78$ cm^{-1} (or $J/k_B = -2.56$ K) and $g = 2.15$ for **6**, $J = -7.88$ cm^{-1} (or $J/k_B = -11.3$ K) and $g = 2.08$ for **7**, and $J = -6.58$ cm^{-1} (or $J/k_B = -9.46$ K) and $g = 2.12$ for **8**. For **5**, **7**, and **8** the agreement between the calculated and experimental data is excellent; the average exchange constants J are antiferromagnetic, leading to an $S = 1/2$ for each isolated [Cu_3] unit. In the case of **6** the

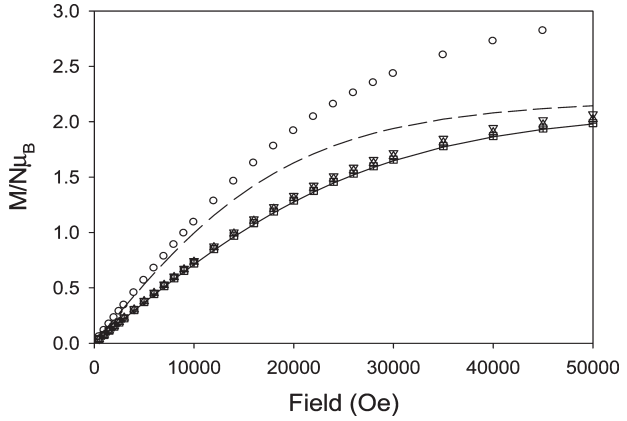

Figure 11. Magnetization vs field plots for complexes **5** (▼), **6** (○), **7** (□), and **8** (Δ) at 2 K.

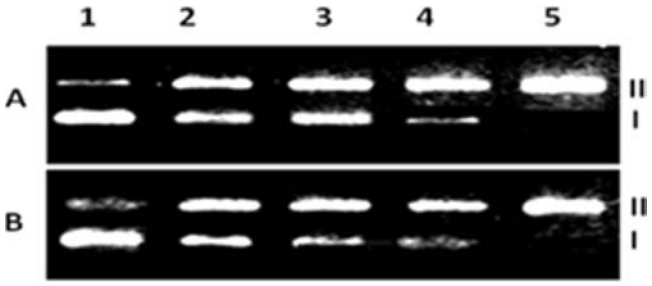

Figure 12. DNA cleavage experiment mediated by **2** and **4** (complex **2** corresponds to gel A and **4** gel B) at different time intervals. Lane 1: DNA alone; lane **2**−**5**: DNA + complex **2** or **4** (5, 10, 15, and 20 min, respectively).

agreement with this model is poor, especially in the low temperature region, indicating the importance of the interaction between the [Cu_3] units through the 4,4′-bpy linkers, which leads to an $S_T = 1$ spin ground state with the excited states very low lying in energy. The two trinuclear Cu units are linked by two 4,4′-bipyridine ligands in which the two aromatic rings are coplanar, providing a pathway for the magnetic exchange through the π system, which provides an affective magnetic exchange pathway between the two trinuclear units. All of the interactions in the complex should be antiferromagnetic, including that through the 4,4′-bpy linker (usually these interactions are weak and antiferromagnetic, of the order of -1 or -2 cm^{-1}),[20] and the $S_T = 1$ spin ground state observed is achieved by competing interactions. The [Cu_3] units of **7** are also linked by two 4,4′-bpy ligands, but in this case the two aromatic rings of the linker are not coplanar, that is, the torsion angle between them is 22°; thus, these linkers cannot provide a good pathway for magnetic exchange, and in fact, the magnetic properties of **7** are better understood as isolated [Cu_3] units. The case is similar for **5** and **8**.

The field dependence of the magnetization at 2 K was studied for all the samples. The magnetization versus field plots are shown in Figure 11. The solid line is the Brillouin function for two $S = 1/2$ complexes with $g = 2.10$, and the dashed line is the Brillouin function for one $S = 1$ complex with $g = 2.10$. The data for **6** does not reach saturation, not even at the highest field of 5 T, indicating an $S_T = 1$ spin ground state with low lying excited states. The magnetization data for **5**, **7**, and **8** reaches saturation at a value of 2 μ_B, but the data is always below the Brillouin curve for an $S_T = 1$ complex, in fact it is better modeled by the Brillouin function for two isolated $S = 1/2$ complexes with $g = 2.1$, in agreement with the susceptibility data and the structural features of this series of hexanuclear Cu(II) complexes.

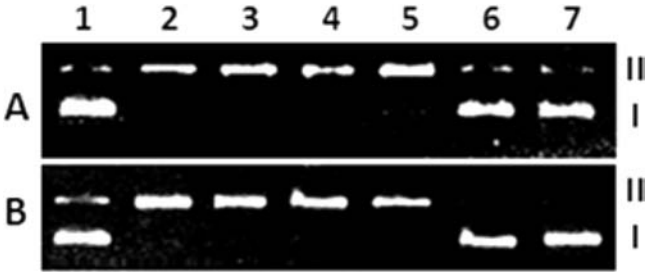

Figure 13. pBR322 cleavage experiments in presence of free radical scavengers and singlet oxygen quencher assisted by complexes **2** and **4** (complex **2** corresponds to gel A and **4** gel B) in a 20 min reaction. Lane 1, DNA alone; lane 2, pBR322+ **2** and **4**; lane 3, pBR322 + **2** and **4** + *tert*-BuOH; lane 4, pBR322 + **2** and **4** + D-Manitol; lane 5, pBR322 + **2** and **4** + DMSO, lane 6, pBR322 + **2** and **4** + NaN_3; lane 7, pBR322 + **2** and **4** + EDTA.

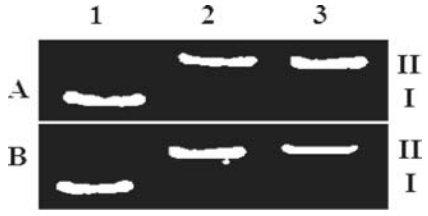

Figure 14. pBR322 DNA cleavage in anaerobic conditions by **2** and **4** (complex **2** corresponds to gel A, **4** to gel B) at 20 min intervals. Lane 1, DNA alone; lanes 2−3, DNA + complex (**2** and **4**).

These results are in good agreement with related compounds containing the phosphonato ligand in its η^3-*O*,*O*′, *O*″ coordination mode, for which superexchange interactions are typically in the range of -5 to -10 cm^{-1}.[15,20,22]

Cleavage of Plasmid DNA. We have systematically examined the DNA cleavage ability[23] of the complexes **2** and **4** (Figure 12). Time course experiments reveal that **2** and **4** were able to mediate complete conversion of the supercoiled pBR322 DNA form I to nick form II in 20 min.

DNA Cleavage Mechanism. Copper-based artificial nucleases function through oxidative and/or hydrolytic pathways. In view of this, we probed the cleavage mechanism of **2** and **4**. In presence of EDTA, the cleavage reaction is completely inhibited demonstrating a crucial role of copper for plasmid modification. Hydroxyl radical

(22) (a) Fernández-Botello, A.; Escuer, A.; Solans, X.; Font-Bardía, M.; Holý, A.; Sigel, H.; Moreno, V. *Eur. J. Inorg. Chem.* **2007**, 1867. (b) Doyle, R. P.; Kruger, P. E.; Moubaraki, B.; Murray, K. S.; Nieuwenhuyzen, M. *Dalton Trans.* **2003**, 4230.

(23) (a) Srivatsan, S. G.; Parvez, M.; Verma, S. *J. Inorg. Biochem.* **2003**, *97*, 340. (b) Chandrasekhar, V.; Deria, P.; Krishnan, V.; Athimoolam, A.; Singh, S.; Madhavaiah, C.; Srivatsan, S. G.; Verma, S. *Bioorg. Med. Chem. Lett.* **2004**, *14*, 1559. (c) Chandrasekhar, V.; Nagendran, S.; Azhakar, R.; Kumar, R. M.; Srinivasan, A.; Ray, K.; Chandrashekar, T. K.; Madhavaiah, C.; Verma, S.; Priyakumar, U. D.; Sastry, N. G. *J. Am. Chem. Soc.* **2005**, *127*, 2410. (d) Chandrasekhar, V.; Athimoolam, A.; Krishnan, V.; Azhakar, R.; Madhavaiah, C.; Verma, S. *Eur. J. Inorg. Chem.* **2005**, *8*, 1482.

scavengers, dimethyl sulphoxide (DMSO), D-mannitol, or *tert*-butylalcohol do not inhibit cleavage reactions demonstrating that radicals are not involved in the cleavage process. NaN_3 is a well-known quencher of singlet oxygen.[24] NaN_3 inhibits the cleavage reaction, which indicates that singlet oxygen may be involved in the cleavage process (Figure 13). However, hydrolytic pathway for plasmid modification also appears potent in the current instance as demonstrated by the fact that DNA cleavage does not decrease under anaerobic conditions (Figure 14). Thus, it appears that multiple reaction pathways may be involved in the plasmid cleavage activity mediated by **2** and **4**.

Conclusion

In conclusion, we have been able to prepare molecular copper(II) phosphonates where the nuclearity of the assembly varies from three to six. Three different structural types involving trinuclear, tetranuclear, and hexanuclear assemblies are accessible from a synthetic protocol involving a Cu(II) salt, a phosphonic acid, and ancillary nitrogen ligands. Use of chelating nitrogen ligands is helpful to limit the nuclearity while bridging nitrogen ligands allow coupling of two trimeric units. Magnetic studies of these complexes reveal an antiferromagnetic behavior for all the complexes at low temperatures. The trinuclear complexes have been investigated for their nuclease activity and have been shown to be excellent plasmid-modifiers even in the absence of external oxidants. It would be interesting to extend the general synthetic principles delineated in this work to other transition metal assemblies. Work in this direction is in progress.

Acknowledgment. We thank the Department of Science and Technology, India, and the Council of Scientific and Industrial Research, India, for financial support. V.C. is a Lalit Kapoor Chair Professor of Chemistry. V.C. is thankful for the Department of Science and Technology, for a J.C. Bose fellowship. T.S. thanks the Council of Scientific and Industrial Research, India, for a Senior Research Fellowship. E.C.S. acknowledges financial support by the Spanish Ministerio de Ciencia e Innovación (Juan de la Cierva Fellowship). R.C. thanks the CNRS, the University of Bordeaux, MAGMANet (NMP3-CT-2005-515767), and the Conseil Régional d'Aquitaine for financial support.

Supporting Information Available: Further details are given in Tables S1−S2 and Figures S1−S13. This material is available free of charge via the Internet at http://pubs.acs.org.

(24) (a) Fortner, A.; Wang, S.; Darbha, G. K.; Ray, A.; Yu, H.; Ray, P. C.; Kalluru, R. R.; Kim, C. K.; Rai, V.; Singh, J. P. *Chem. Phys. Lett.* **2007**, *434*, 127. (b) Macias, B.; Villa, M. V.; Sanz, F.; Borras, J.; Gonzalez-Alvarez, M.; Alzuet, G. *J. Inorg. Biochem.* **2005**, *99*, 1441. (c) Patra, A. K.; Dhar, S.; Nethaji, M.; Chakravarty, A. R. *Chem. Commun.* **2003**, *13*, 1562. (d) Li, Y.; Trush, M. A. *Carcinogenesis* **1993**, *14*, 1303.